Impact Cratering: The Mineralogical and Geochemical Evidence

Christian Koeberl
University of Vienna
Vienna, Austria

ABSTRACT.—Over the past 15 years, new studies related to the events that caused the extinction of the majority of life on Earth at the end of the Cretaceous Period have led to the hypothesis that a large-scale asteroid or comet impact occurred at 65 Ma. In the past, impact cratering as a geologic process has not been much appreciated by the general geological community, despite the fact that, on all other planets and satellites with a solid surface, impact cratering is the most important process that alters the surface at the present time as well as during most of the history of the solar system. Detailed studies, mainly since the 1960s, have led to the recognition of about 150 impact structures on Earth. Here, some fundamental mineralogical and geochemical properties of impact-derived rocks that are used to recognize impact craters are reviewed. The formation of impact craters leads to pressure and temperature conditions in the target rocks that are significantly different from those reached during any internal terrestrial process. Among the most characteristic changes induced by the impact-generated shock waves are irreversible changes in the crystal structure of rock-forming minerals, such as quartz and feldspar. These shock-metamorphic effects are characteristic of impact and do not occur in natural materials formed by any other process. In addition, geochemical methods are used to find traces of the meteoritic projectile in impact-melt rocks and glasses. A complete and diligent mineralogical, petrological, and geochemical study is necessary before any conclusions regarding an impact origin of geologic structures can be reached.

INTRODUCTION

During the 1980s and early 1990s, a lively debate was held in the geological community regarding the cause of the mass extinction that marks the end of the Cretaceous Period, at the Cretaceous/Tertiary (K/T) boundary (see, e.g., Silver and Schultz, 1982; Sharpton and Ward, 1990). Interest in the events at the K/T boundary was renewed by a publication by Alvarez and others (1980), who found that the concentrations of the rare platinum-group elements (PGEs: Ru, Rh, Pd, Os, Ir, and Pt) and other siderophile elements (e.g., Co, Ni) are enriched by up to four orders of magnitude in the thin clay layer marking the K/T boundary compared to their concentrations in normal terrestrial crustal rocks. These observations were interpreted by Alvarez and others (1980) as the result of a large asteroid or comet impact, which caused extreme environmental stress. This hypothesis was later strongly supported by the finding of shocked minerals in the K/T boundary layer by Bohor and others (1984,1987). It turned out that one of the main problems impeding the acceptance of the theory that a large impact took place at 65 Ma was a lack of detailed knowledge of impact cratering and shock-metamorphic processes in the general geological community. Similar debates—regarding impact vs. internal origin—have been held in discussing the origin of a variety of "unusual" structures around the world, including the Ames structure in Oklahoma. Thus, it seems useful to briefly review the basic knowledge of terrestrial impact craters and shock metamorphism. The discussion of general properties of impact craters is the topic of the paper by Grieve (1997), and here I will review mainly mineralogical and geochemical aspects of impact structures.

Historically, the concept of impact cratering on Earth has not been much accentuated in classical geological studies. The concept of classical Huttonian and Lyellian geology is that slow, endogenic

Christian Koeberl, Institute of Geochemistry, University of Vienna, Althanstrasse 14, A-1090 Vienna, Austria.

Koeberl, Christian, 1997, Impact cratering: the mineralogical and geochemical evidence, *in* Johnson, K. S.; and Campbell, J. A. (eds.), Ames structure in northwest Oklahoma and similar features: origin and petroleum production (1995 symposium): Oklahoma Geological Survey Circular 100, p. 30–54.

processes lead to gradual changes in the geologic record. In this uniformitarian view, internal forces are preferred over seemingly more exotic processes to explain geologic phenomena that often give the impression of occurring over very long periods of time. In contrast, impact appears as an exogenic, relatively rare, violent, and unpredictable event, which violates every tenet of uniformitarianism. The explanation of craters on the Moon or Earth as being of impact origin has been opposed by many geologists over much of this century. It is almost ironical that it was Alfred Wegener who published a little-known study (Wegener, 1921), in which he concluded that the craters on the Moon are of meteorite-impact origin. The history of study and acceptance of impact cratering over this century is somewhat similar to the record of the acceptance of plate tectonics (for a historical account of impact-crater studies, see, e.g., Mark, 1987; Hoyt, 1987; Marvin, 1990; and Glen, 1994).

Planetary exploration and extensive lunar research in the second half of the 20th century led to the conclusion that essentially all craters visible on the Moon (and many on Mercury, Venus, and Mars) are of impact origin. Therefore, it has to be concluded that, over its history, the Earth was subjected to a larger number of impact events than the Moon. Part of the reason why this conclusion was not widely accepted among geologists may be that terrestrial processes (weathering, plate tectonics, etc.) effectively work to obliterate the surface expression of these structures on Earth. Through studies of the orbits of asteroids and comets, astronomers have a relatively good understanding of the rate with which these objects strike the Earth (e.g., Shoemaker and others, 1990; Weissman, 1990). For example, minor objects in the solar system with diameters of ≥1 km (mainly asteroids) collide with the Earth at a frequency of about 4.3 impacts per million years (Shoemaker and others, 1990), and each such impact forms a crater ≥10 km in diameter. Impactors of about 2 km in diameter collide with the Earth about every 1 to 2 million years. Impact of Earth-orbit crossing asteroids dominate the formation of craters on Earth that are smaller than about 30 km in diameter, whereas comet impact probably forms the majority of craters that are larger than about 50 km in diameter (Shoemaker and others, 1990). However, the orbits of asteroids are better known than those of comets, because many of the latter have such long periodicities that no appearance has yet been observed during the time of human civilization.

In an important historical and sociological evaluation of the K/T boundary debates, Glen (1994, p. 52) found that "resistance to the [impact] hypothesis seemed inverse to familiarity with impacting studies." Thus, planetary scientists, astronomers, and meteoriticists have grown accustomed to view "large-body impact as a normal geological phenomenon—something to be expected throughout Earth history—but another group, the paleontologists, is confounded by what appears to be an ad hoc theory about a nonexistent phenomenon" (D. M. Raup in Glen, 1994, p. 147). Thus, it may be concluded that one scientist's uniformitarianism is another scientist's *deus ex machina*.

However, it may be important to consider the time scales involved in this discussion. What geologists have called "uniformitarianism" is the result of integrating individual catastrophes of various magnitudes over a sufficiently long time span. Earthquakes, volcanic eruptions, landslides, etc., are locally devastating if time spans of maybe 20 to 100 yr are concerned, but if the whole world and longer time spans are concerned, these "catastrophes" become part of the "uniformitarian" process of explosive volcanism, earthquake history, or erosion. The bias in what is considered uniformitarian is related to the life span of humans and the human civilization. As large meteorite impacts have not been observed during the last few millennia (with rare exceptions, such as the Tunguska event, which occurred in a remote tundra location of Siberia in 1908—but even this event was too small to produce a crater), such events tend to be neglected when constructing the "uniformitarian" history of the Earth. The falls of small meteorites have been observed quite frequently. There is no real conflict between uniformitarianism and meteorite impact. We just have to learn to apply the same principle that is being used for extrapolating the frequency of volcanic eruptions and earthquakes to the scaling of meteorite impacts—the large and devastating ones occur less often than the small events.

About 150 impact structures are currently known on Earth (e.g., Grieve and Shoemaker, 1994; Grieve, 1997). However, it is somewhat embarrassing that almost two thirds of the confirmed or probable impact craters in the United States have only been studied superficially (see Koeberl and Anderson, 1996). Considering that some impact events severely affected the geologic and biological evolution on Earth and that even small impacts can disrupt the biosphere and lead to local devastation (Chapman and Morrison, 1994), the understanding of impact structures and the processes by which they form should be of interest not only to earth scientists, but also to society in general.

GENERAL CHARACTERISTICS OF IMPACT CRATERS

As no large impact event has been observed by humans over the past several thousand years (which is, of course, not a geologically long period of time), impact experiments and the detailed study of impact craters on Earth are essential to understand these features. During an impact event, the geologic structure of the target area is changed in a characteristic way, which can be used

to help distinguish volcanic structures from meteorite impact craters. Meteorite impact craters are circular surficial features without deep roots, whereas in volcanic structures the disturbances continue to (or, rather, emerge from) great depth. Impact craters are practically always circular, with only very few exceptions that result either from highly oblique impacts (see, e.g., the Rio Cuarto structures in Argentina—Schultz and others, 1994) or from postformational distortion due to, for example, tectonism or erosion (e.g., the Sudbury structure in Canada—e.g., Stöffler and others, 1994). It is useful to distinguish between the impact crater, i.e., the feature that results from the impact, and the impact structure, which is what is observed today, long after formation and modification of the crater.

Impact craters (before erosion) occur in two distinctly different morphological forms, namely as small (≤4-km-diameter) bowl-shaped craters and large (≥4-km-diameter) complex craters with a central uplift. All craters have an outer rim and some crater infill (e.g., brecciated and/or fractured rocks, impact-melt rocks), whereas the central structural uplift in complex craters consists of a central peak or of one or more peak ring(s) and exposes rocks that are uplifted from considerable depth. The diameters of impact craters on Earth show a variation, which is, however, the result of biased processes, chiefly different effects of age and differential erosion of large and small craters. The erosional processes that obliterate small (0.5- to 10-km-diameter) craters after a few million years create a severe deficit of these craters, compared to the number that is expected from the number of larger craters and astronomical observations (Grieve and Shoemaker, 1994). Erosion also explains why most small craters are young. Older craters of larger initial diameter also suffer erosion degradation leading to the destruction of the original topographical expression or to burial of the structures under postimpact sediments. For details on crater morphology, see Grieve (1997).

RECOGNITION OF IMPACT STRUCTURES

As a consequence of the obliteration, burial, or destruction of impact craters on Earth, they can be difficult to recognize, requiring the development of diagnostic criteria for the identification and confirmation of impact structures. The most important of these characteristics are (1) evidence for shock metamorphism, (2) crater morphology, (3) geophysical anomalies, and (4) the presence of meteorites or geochemical discovery of traces of the meteoritic projectile. Of these, only the presence of diagnostic shock-metamorphic effects and, in some cases, the discovery of meteorites, or traces thereof, can provide unambiguous evidence for an impact origin.

However, morphological and geophysical observations are important in providing supplementary—but not confirming—evidence. Geophysical methods are also useful in identifying candidate sites for further studies. It should be noted that in complex craters, the central uplift usually contains severely shocked material and is often more resistant to erosion than the rest of the crater. In old eroded structures, the central uplift may be the only remnant of the crater that can be identified. Geophysical characteristics of impact craters that have been investigated include gravity, magnetic properties, reflection and refraction seismic signatures, electrical resistivity, and others (see Pilkington and Grieve, 1992, for a review). In general, simple craters have negative gravity anomalies due to the lower density of the brecciated rocks compared to the unbrecciated target rocks, whereas complex craters often have a positive gravity anomaly associated with the central uplift that is surrounded by an annular negative anomaly. Magnetic anomalies can be more varied than gravity anomalies, but seismic data show the loss of seismic coherence due to structural disturbance, slumping, and brecciation. Such geophysical surveys are important for the recognition of anomalous subsurface structural features, which may be deeply eroded craters or simply covered by postimpact sedimentary deposits (e.g., in the United States: Ames, Avak, Chesapeake Bay, Manson, Newporte, Red Wing Creek—see Koeberl and Anderson, 1996; Koeberl and Reimold, 1995a,b; Koeberl and others, 1995b,1996b,c). However, to better appreciate the other criteria for identification of impact structures, it is necessary to briefly consider some physical processes that operate during crater formation.

FORMATION OF IMPACT CRATERS

The formation of a crater by hypervelocity impact is—not only in geologic terms—a very rapid process that is usually divided into three stages: (1) contact and compression stage, (2) excavation stage, and (3) postimpact crater-modification stage. Crater-formation processes have been studied for many decades, but space limitations require that the reader be referred to the literature (see, e.g., Gault and others, 1968; Roddy and others, 1977; Melosh, 1989; and references therein) for a detailed discussion of the physical principles of impact-crater formation. Here, only a few key ideas can be mentioned.

During the impact of a large meteorite, asteroid, or comet, large amounts of kinetic energy (equal to $\frac{1}{2}\,mv^2$, m = mass, v = velocity) are released. Earlier in the century, the amount of energy was largely underestimated, because the velocities with which extraterrestrial bodies hit the Earth had not been known or assessed properly. However, any body that is not slowed down by the atmosphere will hit the Earth with a velocity be-

tween about 11 and 72 km/s. These velocities are determined by celestial mechanics. Thus, a 250-m-diameter iron or stony meteorite has a kinetic energy roughly equivalent to about 1,000 megatons of TNT, which would lead to the formation of a crater about 5 km in diameter. The relatively small Meteor (or Barringer) crater in Arizona (1.2 km diameter) was produced by an iron meteorite with a diameter of about 30 to 50 m. Many of the characteristics of an impact crater are the consequence of the enormous kinetic energy that is released almost instantaneously during the impact. This energy can be compared to that of "normal" terrestrial processes, such as volcanic eruptions or earthquakes. During small impact events, which may lead to craters of 5 to 10 km diameter, about 10^{24} to 10^{25} ergs (10^{17} to 10^{18} J) are released, whereas during formation of larger craters (50 to 200 km diameter), about 10^{28} to 10^{30} ergs (10^{21} to 10^{23} J) are liberated (e.g., French, 1968; Kring, 1993). On the other hand, about $6 \cdot 10^{23}$ ergs ($6 \cdot 10^{16}$ J) were released over several months during the 1980 eruption of Mount St. Helens, and 10^{24} ergs (10^{17} J) in the big San Francisco earthquake in 1906. It may also be surprising that the total annual energy release from the Earth (including heat flow, which is by far the largest component, as well as volcanism and earthquakes) is about $1.3 \cdot 10^{28}$ ergs ($1.3 \cdot 10^{21}$ J/yr) (French, 1968; Sclater and others, 1980; Morgan, 1989). The latter amount of energy is comparable to the energy that is released almost instantaneously during large impact events. It is also important to realize that the energy that is liberated during an impact is concentrated at almost a point on the Earth's surface, leading to an enormous local energy density.

SHOCK WAVES IN ROCKS—HUGONIOT EQUATIONS

Structural modifications and phase changes in the target rocks occur during the compression stage, and the morphology of a crater is defined in the second and third stage. For a more detailed description of crater formation, see, e.g., Grieve (1987,1991), Melosh (1989), and references therein. During the early-impact phase, the impacting body is stopped after about two projectile radii, and the kinetic energy ($\frac{1}{2} mv^2$) is transformed into heat and shock waves that penetrate into the projectile and target. The most important phenomenon, which is characteristic of impact, is the generation of a supersonic shock wave that is propagated into the target rock. The effects of shock waves on matter are well understood from decades of experimental evidence. The following discussion is based mainly on information from Melosh (1989). Matter is being accelerated very rapidly, and, as a consequence of the decrease of compressibility with increasing pressure, the resulting stress wave will become a shock wave moving initially at supersonic speed (up to about ⅔ of the impact velocity). Shock waves are inherently nonlinear and shock fronts are abrupt. They can be mathematically represented as a discontinuous jump of pressure, density, particle velocity, and internal energy. In reality, shock waves have a finite thickness, which is, however, very limited. For example, the widths of shock waves in gas are limited to about 10 μm, which is roughly equal to one molecular mean free path, but shock waves in solids are wider, up to a few meters in rocks, depending on their porosities.

The shock wave leads to compression of the target rocks at pressures far above a material property called the Hugoniot elastic limit. The Hugoniot elastic limit (HEL) can generally be described as the maximum stress that can be reached in a stress wave that a material can be subjected to without permanent deformation. Above this limit, plastic, or irreversible, distortions occur in the solid medium through which the compressive wave travels (see, e.g., compilations by Roddy and others, 1977; Melosh, 1989; and references therein). The value of the HEL is about 5 to 10 GPa for most minerals and whole rocks. For example, single crystals of quartz have HELs ranging from 4.5 to 14.5 GPa (depending on the crystal orientation); for feldspar the HEL is at 3 GPa, and for olivine it is at 9 GPa. For rocks, the HEL of dolomite is 0.3 GPa, for granite 3 GPa, and for granodiorite, 4.5 GPa. The only known process that produces shock pressures exceeding the HELs of most crustal rocks and minerals in nature is impact cratering. Volcanic processes are not known to exceed 0.5 to 1 GPa. In addition to structural changes, phase changes may occur as well.

For a thermodynamics treatment of shock fronts traveling through matter, the so-called Hugoniot equations are used (see Melosh, 1989). These equations link the pressure P, internal energy E, and density ρ in front of a shock wave (uncompressed: P_0, E_0, ρ_0) to values after the shock front (compressed: P, E, ρ). The density is also expressed as the specific volumes $V = 1/\rho$ and $V_0 = 1/\rho_0$ for the compressed and uncompressed cases, respectively. Initial pressure, energy, and density before the shock are known values, whereas the values after the shock are unknown quantities, as are the shock velocity U and particle velocity u_p behind the shock front. The Hugoniot equations are then written as

$$\rho(U - u_p) = \rho_0 U$$

$$P - P_0 = \rho_0 u_p U$$

$$E - E_0 = (P + P_0)(V_0 - V)/2.$$

These equations express the conservation of mass, momentum, and energy across the shock front to reduce the number of unknown variables from five to two. For a derivation of the Hugoniot equations, see appendix 1 in Melosh (1989) as well as Boslough and Asay (1993). In the uncompressed material, the initial particle velocity should be

zero, and the initial pressure P_0 can be neglected, yielding the approximation $E - E_0 = u_p^2/2$. In addition to the three equations mentioned above, a fourth one, the equation of state, is necessary to specify conditions on either side of the shock front. This equation links pressure, specific volume (density), and internal energy: P = (V,E). Equations of state have been determined experimentally for a large number of different materials (e.g., Marsh, 1980).

The shock-wave equation-of-state data can be plotted in pressure vs. specific-volume (Fig. 1) or shock-velocity vs. particle-velocity diagrams. The curves in these diagrams are not equivalent to conventional equilibrium in thermodynamics P,V diagrams, but represent loci of several individual shock events, i.e., each point on a curve is the result of one particular shock-wave compression event. The HEL appears as a kink in the shock curve, indicating yielding at the maximum stress of the elastic wave (Fig. 1).

After the shock wave passes, the high pressure is released by a so-called rarefaction, or release, wave, which trails the shock front. The rarefaction wave is a pressure, not shock, wave and travels at the speed of sound in the shocked material. It gradually overtakes the decaying shock front and causes a decrease in pressure with increasing distance of propagation. Although the pressure behind a rarefaction wave may drop to near zero, the residual particle velocity actually accelerates material, leading to impact-crater excavation. In addition, the rarefaction wave not only conserves mass, energy, and momentum (as the shock wave does), but also entropy. Thus, rarefaction is a thermodynamically reversible adiabatic process, whereas shock compression is thermodynamically irreversible. During shock compression, a large amount of energy is being introduced into a rock. Upon decompression, the material follows a release adiabat in a pressure vs. specific-volume diagram. The release adiabat is located close to the Hugoniot curve, but usually at generally somewhat higher P and V values, leading to excess heat appearing in the decompressed material, which may result in phase changes (e.g., melting or vaporization). The effects of the phenomena described above can be observed in various forms in shocked minerals and rocks.

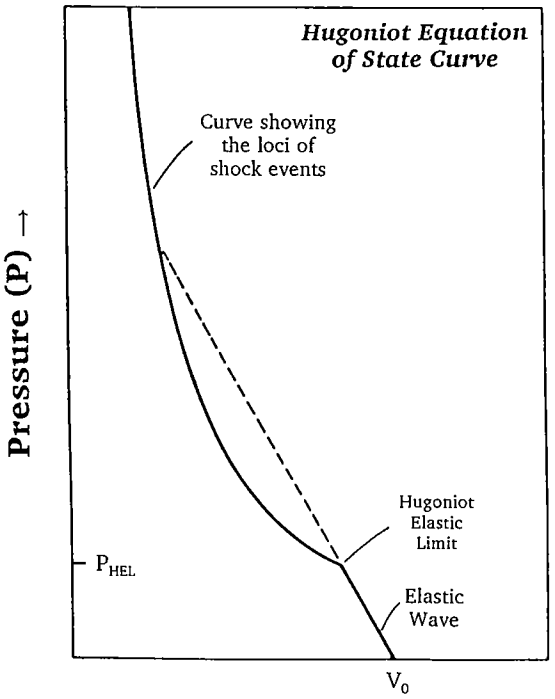

Figure 1. Idealized representation of a Hugoniot equation of state curve. The Hugoniot curve does not represent a continuum of states as in thermodynamics diagrams, but the loci of individual shock-compression events. The yielding of the material at the Hugoniot elastic limit is indicated. See text for detailed discussion.

SHOCK METAMORPHISM

A large meteorite impact will produce shock pressures of ≥100 GPa and temperatures of ≥3,000 °C in large volumes of the target rock. These conditions are in sharp contrast to conditions for endogenic metamorphism of crustal rocks, with maximum temperatures of 1,200 °C and pressures of usually <2 GPa (except static pressure affecting some deep-seated rocks, e.g., eclogites) (Fig. 2). As mentioned above, shock compression is not a thermodynamically reversible process, and most of the structural and phase changes in mineral crystals and rocks are uniquely characteristic of the high pressures (5 to >50 GPa) and extreme strain rates (106 to 108 s^{-1}) associated with impact. Also, some assemblages of high-pressure and high-temperature mineral phases are preserved together with glass in shocked rocks due to disequilibrium caused by transient high pressures followed by quenching.

As some recent literature indicates, there is still some incomplete understanding in the geological community about the precise nature of shock metamorphism (for a discussion, see, e.g., French, 1990; Sharpton and Grieve, 1990). In contrast to some assertions (e.g., Lyons and others, 1993), the existence of definite shock-metamorphic features in volcanic rocks has never been substantiated (see, e.g., de Silva and others, 1990; Gratz and others, 1992b). Static compression, as well as volcanic or tectonic processes, yields different products because of lower peak pressures and because of strain rates that are smaller by more than 11 orders of magnitude. It should be reaffirmed

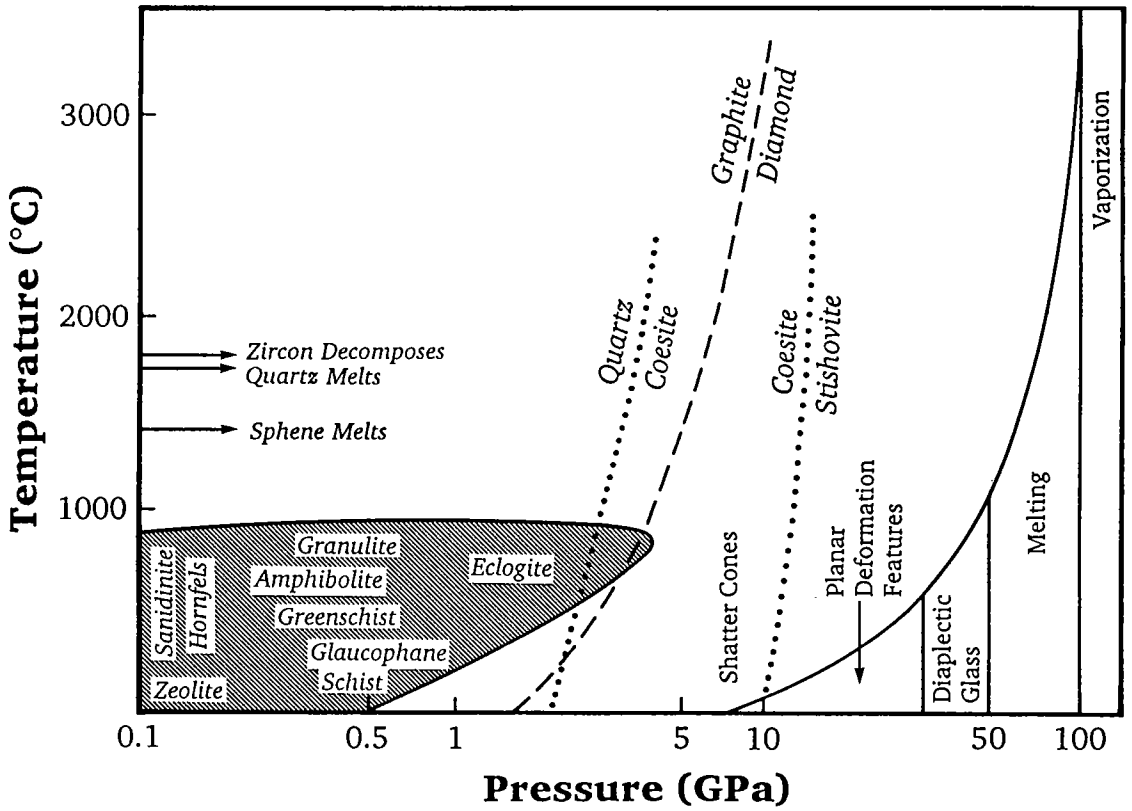

Figure 2. Comparison of pressure-temperature fields of endogenic metamorphism and shock metamorphism. Also indicated are the onset pressures of various irreversible structural changes in the rocks due to shock metamorphism. The curve on the right side of the diagram shows the relationship between pressure and postshock temperature for shock metamorphism of granitic rocks. (After Grieve, 1987, and B. M. French, personal communication, 1995.)

that the study of the response of materials to shock is not a recent development, but has been the subject of thorough investigations over several decades, in part stimulated by military research. Numerous shock-recovery experiments (i.e., controlled shock-wave experiments, which allow the collection of the shocked samples for further studies), using various techniques, have been performed in the past three to four decades. These experiments have led to a good understanding of the conditions for formation of shock-metamorphic products and a pressure-temperature calibration of the effects of shock pressures up to about 100 GPa (see, e.g., Hörz, 1968; French and Short, 1968; Stöffler, 1972,1974; Gratz and others, 1992a,b; Huffman and others, 1993; Stöffler and Langenhorst, 1994; and references therein).

Table 1 lists the most characteristic products of shock metamorphism, as well as the associated diagnostic features. The best diagnostic indicators for shock metamorphism are features that can be studied easily by using the polarizing microscope. They include planar microdeformation features; optical mosaicism; changes in refractive index, birefringence, and optical axis angle; isotropization; and phase changes.

Before discussing the various shock-metamorphic features, the type and location of impactite lithologies should be mentioned (Fig. 3). In an impact crater, shocked minerals, impact melts, and impact glasses are commonly found in various impact-derived breccias. Well-preserved ejecta at the crater rim may display a stratigraphic sequence that is inverted compared to the normal stratigraphy in the area. The impact process leads to the formation of various monomict or polymict breccias (e.g., Fig. 4), which are found within and around the resulting crater (see also Stöffler and Grieve, 1994, and Koeberl and others, 1996a). There are three main types: (1) cataclastic (fragmental) breccias, (2) suevitic (fragmental with a melt-fragment component) breccias, or (3) impact-melt (melt breccia—i.e., melt in the matrix with a clastic component) breccias. The breccias can be allochthonous or autochthonous. In addition, dikes of injected or locally formed fragmental or

TABLE 1.—CHARACTERISTICS AND FORMATION PRESSURES OF VARIOUS SHOCK DEFORMATION FEATURES

Pressure (GPa)	Features	Target characteristics	Feature characteristics
2–30	Shatter cones	Best developed in homogeneous, fine-grained, massive rocks	Conical fracture surfaces with subordinate striations radiating from a focal point
5–45	Planar fractures and planar deformation features (PDFs)	Highest abundance in crystalline rocks; found in many rock-forming minerals; e.g., quartz, feldspar, olivine, and zircon	PDFs: Sets of extremely straight, sharply defined parallel lamellae; occur often in multiple sets with specific crystallographic orientations.
30–40	Diaplectic glass	Most important in quartz and feldspar (e.g., maskelynite from plagioclase)	Isotropization through solid-state transformation under preservation crystal habit as well as primary defects and sometimes planar features. Index of refraction lower than in crystal but higher than in fusion glass
15–50	High-pressure polymorphs	Quartz polymorphs (coesite, stishovite) most common but also ringwoodite from olivine, jadeite from plagioclase, and majorite from pyroxene	Recognizable by crystal parameters, confirmed usually with XRD or NMR;[a] abundance influenced by postshock temperature and shock duration; Stishovite is temperature-labile
>35	Impact diamond	From carbon (graphite) present in target rocks; rare	Cubic and hexagonal form; usually very small but occasionally up to millimeter-size; inherit graphite crystal shape
45–>70	Mineral melts	Rock-forming minerals (e.g., lechatelierite from quartz)	Contrary to diaplectic glass, liquid-state transformation of a mineral into glass.
>60	Rock melt	Best developed in massive silicate rocks. Occur as individual melt bodies (millimeter to meter size) or as coherent melt sheets, up to >1000 km^3.	Either glassy (fusion glasses) or crystalline; of macroscopically homogeneous, but microscopically often heterogeneous composition

Data from: Alexopoulos and others (1988), French and Short (1968), Sharpton and Grieve (1990), Stöffler (1972, 1974), Koeberl and others (1995a); after Koeberl (1994).

[a]XRD = X-ray diffraction; NMR = nuclear magnetic resonance.

pseudotachylitic breccias (Reimold, 1995), which contain evidence of melting, can be found in the basement rocks. The schematic distribution of breccias, melt, and breccia dikes at a simple crater is shown in Figure 3. Whether these various breccia types are indeed present in a crater depends on factors including the size of the crater, the composition and porosity of the target area (e.g., Kieffer and Simonds, 1980), and the level of erosion (see, e.g., Roddy and others, 1977; Hörz, 1982; Hörz and others, 1983; Grieve, 1987; and references therein).

Shatter Cones

The occurrence of shatter cones has long been discussed as a good macroscopic indicator of shock effects, and a variety of structures were proposed to be of impact origin on the basis of shatter-cone occurrences (e.g., Dietz, 1968; Milton, 1977). Such cones have also been formed in (chemical) explo-

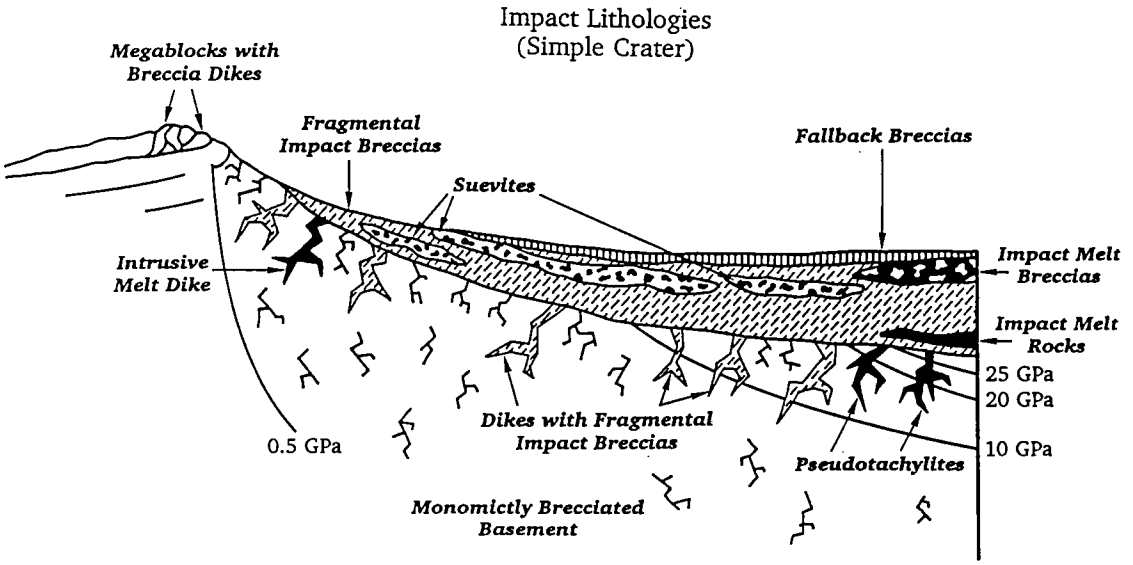

Figure 3. Schematic cross section through a simple impact crater (from the rim on the left side to the crater center on the right side). The various types and locations of occurrence of impactites (i.e., rocks affected during the impact process) are shown. (After Koeberl and Anderson, 1996.)

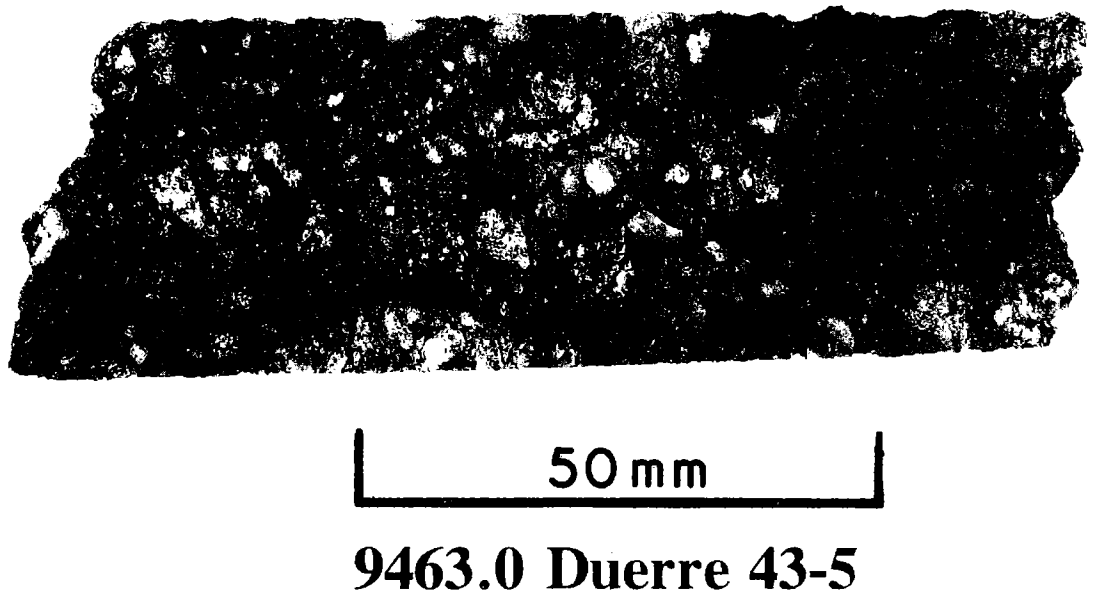

Figure 4. Macroscopic view of a granitic fragmental breccia from the Newporte impact structure, North Dakota; sample D9463.0 from the Shell no. 43-5 Duerre drill core (from 2,884 m depth), showing angular granitic fragments in a dark, fine-grained, clast-rich matrix.

sion crater experiments (see, e.g., Milton, 1977). Their formation is dependent on the type of target rock (i.e., they are better developed in certain lithologies than in others) and has been estimated to take place at pressures in the range of 2 to 30 GPa. In general, shatter cones are cones with regular thin grooves (striae) that radiate from the top (the apex) of a cone. They can range in size from <1 cm to >1 m (Fig. 5). Shatter cones occur mostly in the outer and lower parts of a crater and

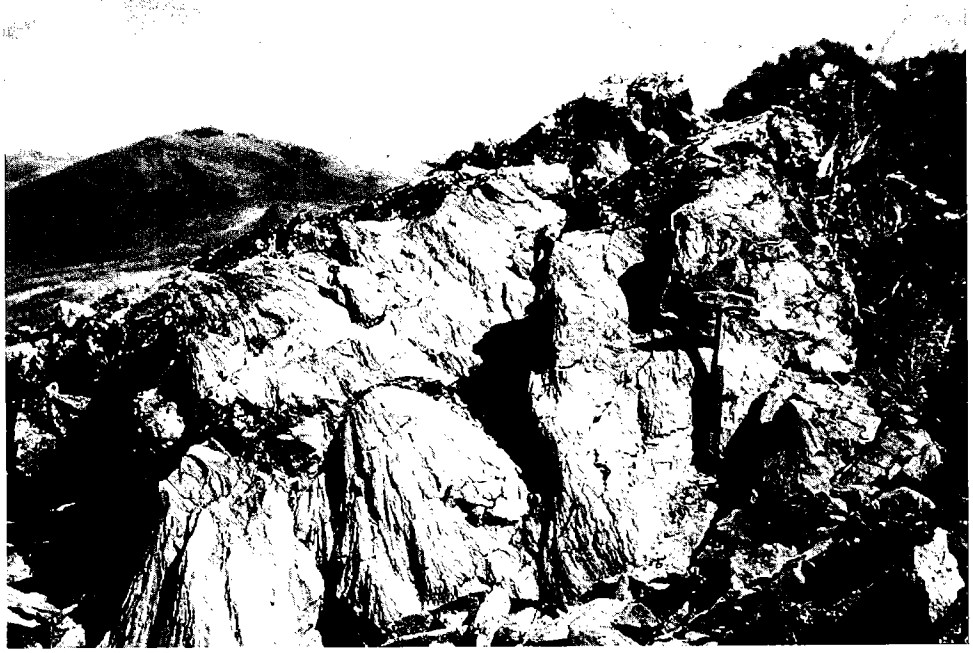

Figure 5. Assemblage of massive shatter cones, with sizes up to 1 m, at the Beaverhead impact structure, Montana (courtesy P. Fiske).

may be preserved even if a structure is deeply eroded. Unfortunately, conclusive criteria for the recognition of "true" shatter cones have not yet been defined. If they are strongly eroded, it is possible to confuse concussion features, pressure-solution features (cone-in-cone structure), or abraded or otherwise striated features with shatter cones. It would be important to arrive at some generally accepted criteria for the correct identification of shatter cones, as some impact craters have been identified almost exclusively by the occurrence of shatter cones (see, e.g., compilation by Koeberl and Anderson, 1996; cf. Koeberl and others, 1996b). However, shatter cones are important potential macroscopic shock indicators, as they are developed in large volumes of rock, and are useful as a guide for the presence of more definitive shock indicators, such as shocked minerals (see below).

Mosaicism

Mosaicism is a microscopic effect of shock metamorphism and appears as an irregular mottled optical extinction pattern (Fig. 6A), which is distinctly different from the undulatory extinction that occurs in tectonically deformed quartz. Mosaicism can be measured in the optical microscope by determining the scatter of optical axes in different regions of crystals showing mosaicism. Mosaicism can be semiquantitatively defined by X-ray diffraction studies of the asterism of single-crystal grains, where it shows up as a characteristic increase (with increasing shock) of the width of individual lattice-diffraction spots in diffraction patterns. Highly shocked quartz crystals show a diffraction pattern that becomes similar to a powder pattern, because of shock-induced polycrystallinity. Many shocked quartz grains that show planar microstructures also show mosaicism. In addition, it should be noted that the crystal lattice of shocked quartz shows lattice expansion above shock pressures of 25 GPa, leading to an expansion of the cell volume by ≤3% (Langenhorst, 1994).

Planar Microstructures

Two types of planar microstructures are apparent in shocked minerals: planar fractures (PFs) and planar deformation features (PDFs). Their characteristics are summarized in Table 2. PDFs in rock-forming minerals (e.g., quartz, feldspar, or olivine) are generally accepted to be diagnostic evidence for shock deformation (see, e.g., French and Short, 1968; Stöffler, 1972,1974; Alexopoulos and others, 1988; Sharpton and Grieve, 1990; Stöffler and Langenhorst, 1994). PFs, in contrast to irregular, nonplanar fractures (which are caused by rarefaction waves), are thin fissures, spaced about 20 μm or more apart, which are parallel to rational crystallographic planes with low

TABLE 2. —CHARACTERISTICS OF PLANAR FRACTURES AND PLANAR-DEFORMATION FEATURES IN QUARTZ

Nomenclature	1. Planar fractures (PF) 2. Planar-deformation features (PDF) 2.1. Nondecorated PDFs 2.2. Decorated PDFs
Crystallographic orientation	1. PFs: usually parallel to (0001) and {10$\bar{1}$1} 2. PDFs: usually parallel to {10$\bar{1}$3}, {10$\bar{1}$2}, {10$\bar{1}$1}, (001), {11$\bar{2}$2}, {11$\bar{2}$1}, {10$\bar{1}$0}, {11$\bar{2}$0}, {21$\bar{3}$1}, {51$\bar{6}$1}, etc.
Optical microscope properties	Multiple sets of PFs or PDFs (up to 15 orientations) per grain Thickness of PDFs: <2–3 μm Spacing: >15 μm (PFs), 2–10 μm (PDFs)
TEM properties (PDFs)	Two types of primary lamellae are observed: 1. Amorphous lamellae with a thickness of about 30 nm (at pressures of <25 GPa) and about 200 nm (at pressures of >25 GPa) 2. Brazil twin lamellae parallel to (0001)

Data after Stöffler and Langenhorst (1994).

Miller indices, such as (0001) or {10$\bar{1}$1} (e.g., Engelhardt and Bertsch, 1969). PFs form at lower pressures than PDFs and may not provide conclusive evidence of shock metamorphism, but can act as guide to other, more characteristic, shock-deformation effects.

PDFs, together with the somewhat less definitive planar fractures (PFs), are well developed in quartz (Stöffler and Langenhorst, 1994). PDFs are parallel zones with a thickness of ≤1 to 3 μm and are spaced about 2 to 10 μm apart (see examples in Fig. 6). The degree of planarity of the individual sets of PDFs is an important parameter for the correct identification of bona fide PDFs and allows their distinction from (sub-)planar features that are produced at lower strain rates, e.g., in tectonically deformed quartz. It was demonstrated in transmission electron microscopy (TEM) studies (see, e.g., Goltrant and others, 1991) that PDFs consist of amorphous silica. The structural state of the glassy lamellae is, however, slightly different from that of regular silica glass (Goltrant and others, 1991). The fact that the PDF lamellae are filled by glass allows them to be preferentially etched by, e.g., hydrofluoric acid, emphasizing the planar-deformation features (see Fig. 6C). The photomicrographs in Figure 6 show various appearances of PDFs in natural samples from impact structures in the United States.

Engelhardt and Bertsch (1969) have classified PDFs into four groups: (1) nondecorated PDFs (extremely fine lamellae, cannot be resolved in the

Figure 6 *(p. 40–41)*. Shocked quartz and feldspar. A—Quartzitic clast in impact-melt rock from the Manson crater, Iowa, showing two prominent sets of PDFs and shock mosaicism (width of field of view, 2.2 mm; crossed polarizers; see Koeberl and others, 1996a). B—Close-up of K-feldspar grain from the Ames structure, Oklahoma, Nicor no. 18-4 Chestnut core, sample 9011.0 (from 2,747 m depth), showing incipient brecciation in the feldspar grain, which contains three sets of PDFs and shows the closely spaced nature of the lamellae (width of field of view, 900 μm; crossed polarizers; courtesy W. U. Reimold, University of the Witwatersrand). C—SEM image of quartz grain from the K/T boundary layer at DSDP Site 596 (Southwest Pacific), after brief etching with HF, showing three different sets of PDFs (courtesy B. Bohor, U.S. Geological Survey). D—Shocked quartz grain from the Red Wing Creek impact structure, North Dakota, from the True Oil 11-27 Burlington Northern borehole, depth interval 2,155 to 2,201 m, within brecciated Kibbey Sandstone, with PDFs of two different orientations (width of field of view, 375 μm; crossed polarizers; see Koeberl and Reimold, 1995a; Koeberl and others, 1996b). E—Quartz grain from the Newporte crater, North Dakota (Koeberl and Reimold, 1995b), with three sets of PDFs, in granitic clast from granitic fragmental breccia D9462.2 (width of field of view, 355 μm; parallel polarizers).

Figure 6A.

Figure 6B.

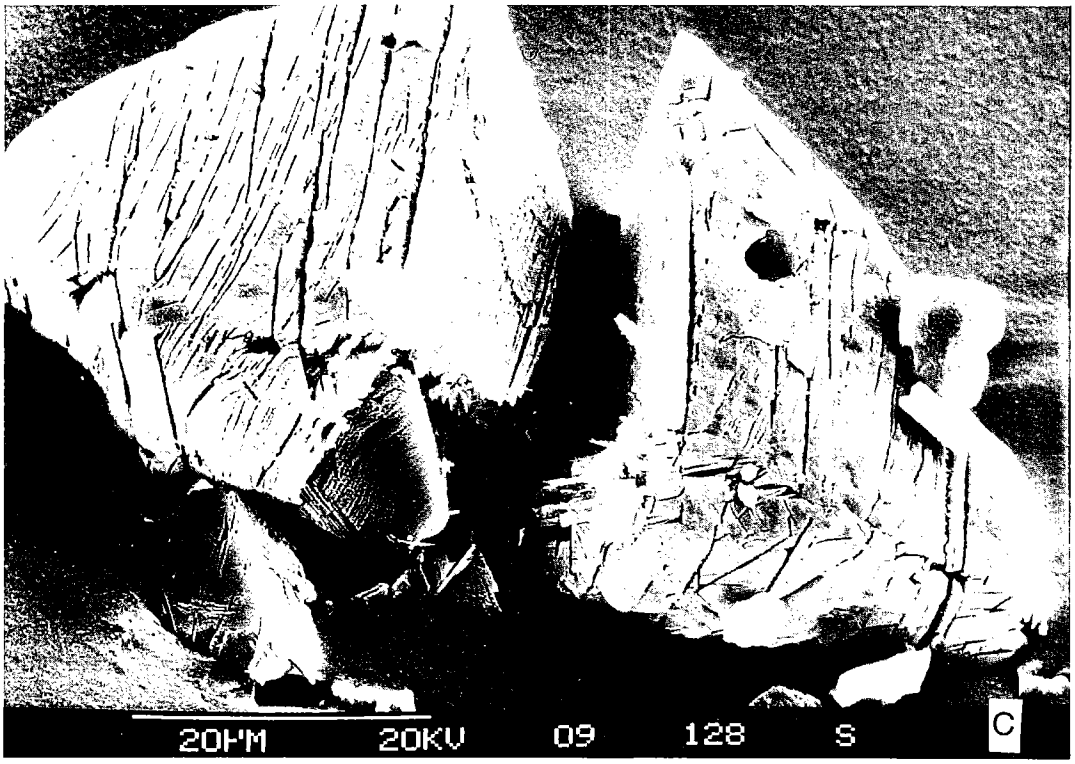

Figure 6C.

Figure 6D.

Figure 6E.

optical microscope), (2) decorated PDFs (the lamellae are lined by, or replaced with, small spherical or elliptical bubbles, often representing fluid inclusions), (3) homogeneous lamellae (thicker lamellae that can be resolved in the microscope), and (4) filled PDFs (where the lamellae are filled with very fine grained crystals). Types 1 and 2 are the most common.

In addition, TEM studies have shown that there is a second type of PDF, which consists of very thin multiple lamellae of Brazil twins. Brazil twins have been observed in hydrothermally grown quartz, but always parallel to the $\{10\bar{1}1\}$ plane, whereas the impact-derived Brazil twins form at pressures of >8 GPa, are of mechanical origin, and are exclusively parallel to the (0001) plane (Goltrant and others, 1991; Leroux and others, 1994). It was shown that such Brazil twins, from the Vredefort impact structure in South Africa, were formed by annealing of the shocked rocks (Goltrant and others, 1991; Leroux and others, 1994).

Most rock-forming minerals, as well as accessory minerals, such as zircon (Fig. 7), develop PDFs. The occurrence of diagnostic shock features is by far the most important criterion for evaluating the impact origin of a crater, particularly when several of the features that are typical of progressive shock metamorphism, as listed in Table 1, have been found. The occurrence of PDFs and PFs can be used, together with other shock effects, to determine the maximum shock pressure in impactites (Fig. 8). Most commonly, quartz is used to study these shock effects, as it is the simplest, best studied, and most widely distributed rock-forming mineral that develops PDFs.

PDFs occur in planes corresponding to specific rational crystallographic orientations. In quartz, the most abundant mineral that develops distinctive PDFs, the (0001) or c (basal), $\{10\bar{1}3\}$ or ω, and $\{10\bar{1}2\}$ or π orientations are the most common ones. In addition, PDFs often occur in more than one crystallographic orientation per grain. With increasing shock pressure, the distances between the planes decrease, and the PDFs become more closely spaced and more homogeneously distributed over the grain, until at about ≥35 GPa, complete isotropization has been achieved. Depending on the peak pressure, PDFs are observed in 2 to 10 (maximum 18) orientations per grain. To properly characterize PDFs, it is necessary to measure their crystallographic orientations by using either a universal stage (Reinhard, 1931; Emmons, 1943) or a spindle stage (Medenbach, 1985), or by using

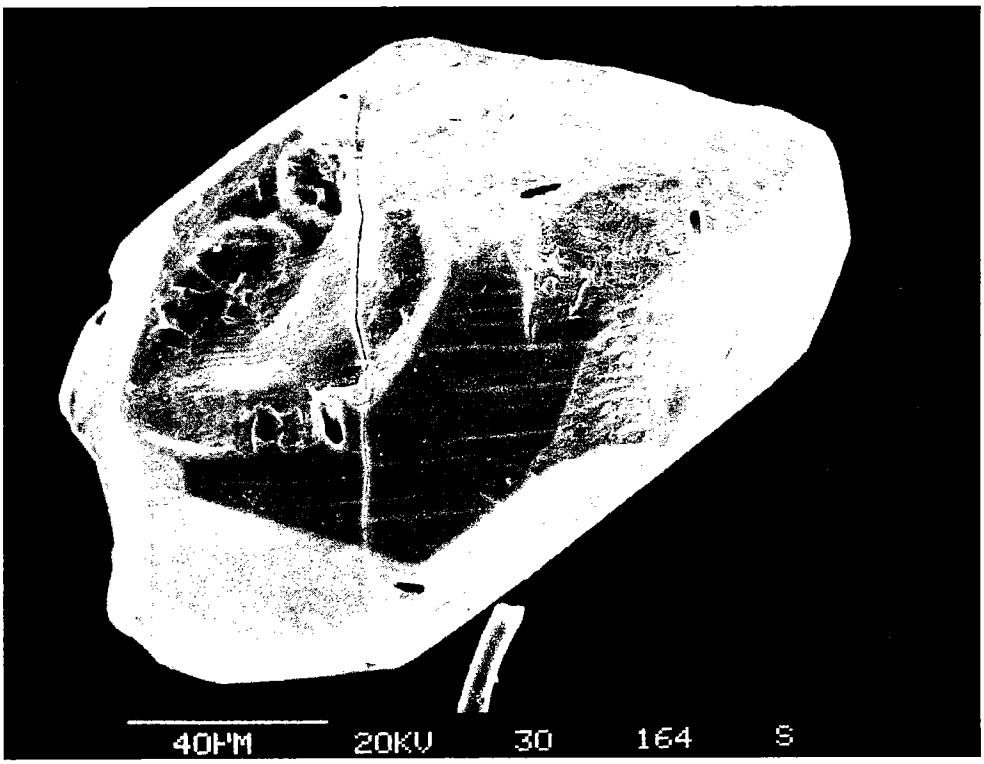

Figure 7. SEM image of an etched shocked-zircon grain from the Berwind Canyon (Raton basin, Colorado, United States) K/T boundary section; the whole grain shows the typical crystal habit of zircon and displays PDFs in two different orientations (courtesy B. Bohor, U.S. Geological Survey).

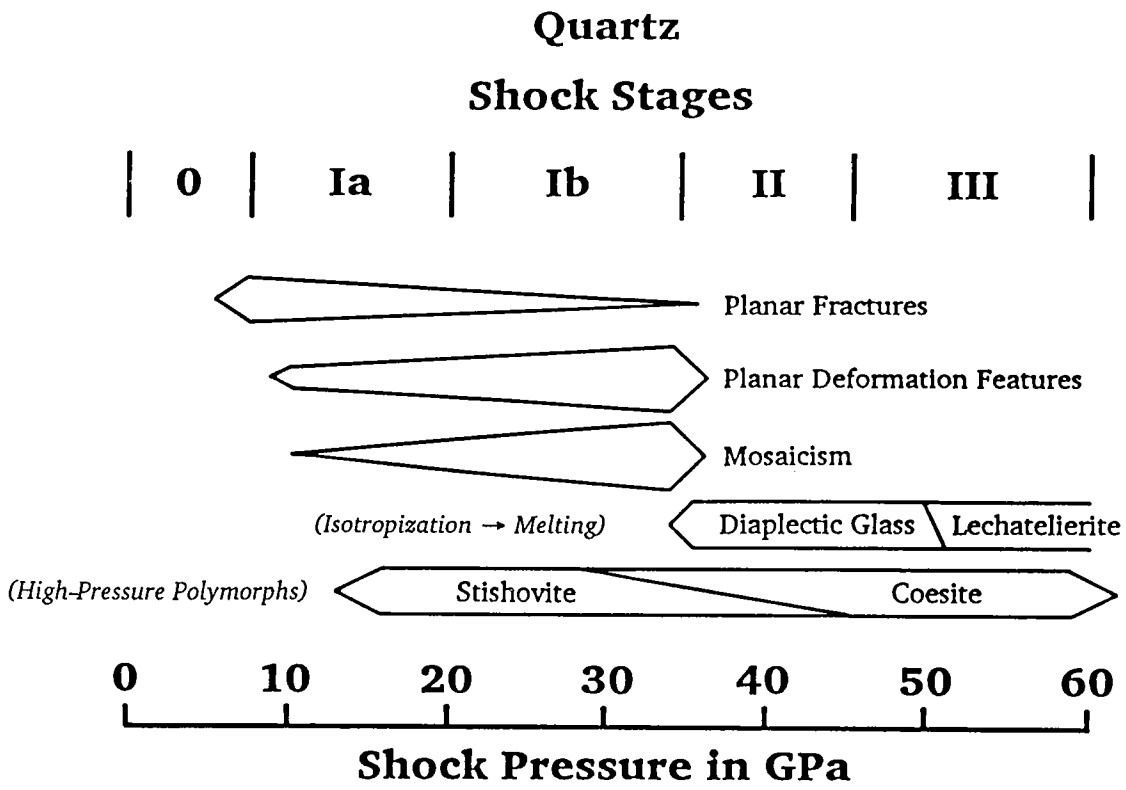

Figure 8. Pressure dependency of various characteristic shock indicators in quartz and relation to shock stages. (After Stöffler and Langenhorst, 1994.)

TEM (see, e.g., Goltrant and others, 1991; Gratz and others, 1992a; Leroux and others, 1994).

It is possible to use the relative frequencies of the crystallographic orientations of PDFs to calibrate shock pressure regimes, as given in Table 3 (see, e.g., Robertson and others, 1968; Hörz, 1968; Stöffler and Langenhorst, 1994). For example, at 5 to 10 GPa, PDFs with (0001) and {10$\bar{1}$1} orientations are formed, whereas PDFs with {10$\bar{1}$3} orientations start to form between about 10 and 12 GPa. Such studies are done by measuring the angles of the c-axis and of the PDFs in individual quartz grains with a universal stage. In a stereographic projection (Fig. 9), the optical axis (c-axis) is rotated into the center of projection, the locations of the poles of PDFs are plotted, and then those positions are compared with the stereographic projection of the rational crystallographic planes in quartz (as listed in Fig. 9). The measured angles that fall within 5° of the theoretical polar angle of the plane are considered valid and can be indexed. Figure 10 shows the results of this procedure in the form of a histographic plot of indexed PDFs. Such plots are used to identify the relative frequencies in which the various shock-characteristic crystallographic orientations occur.

The preshock temperature of a target rock also influences the formation and distribution of PDFs. Reimold (1988) and Huffman and others (1993) presented the results of shock experiments with quartzite both at room temperature (25 °C) and preheated to 450 and 750 °C. They noticed a slight difference in the relative distribution of the {10$\bar{1}$3} and {10$\bar{1}$2} orientations and a large difference in the number of PDF sets per grain (Fig. 11). Langenhorst (1993) compared PDF orientations in shocked quartz single crystals preheated to a higher temperature than Huffman and others (1993) and found a distinct change in the relative frequencies of the {10$\bar{1}$3} and {10$\bar{1}$2} orientations.

Bulk Optical and Other Properties

Recent experimental evidence shows that there is a decrease of the density of shocked quartz with increasing shock pressure (Langenhorst, 1993). At shock pressures up to about 25 GPa, only a slight decrease is noticeable, followed by a significant drop in density between 25 and 35 GPa, depending on the direction of the shock wave relative to the c-axis of the quartz crystal and the preshock temperature (Fig. 12). Optical properties, such as the birefringence of quartz and its refractive index,

TABLE 3.—RELATION BETWEEN SHOCK STAGE AND CRYSTALLOGRAPHIC ORIENTATION (INDICES) OF PLANAR MICROSTRUCTURES IN QUARTZ

Shock stage	Main orientations[a]	Additional orientations	Optical properties
1. Very weakly shocked	PFs: (0001)	PFs: rarely $\{10\bar{1}1\}$ PDFs: none	normal
2. Weakly shocked	PDFs: $\{10\bar{1}3\}$	PFs: $\{10\bar{1}1\}$, (0001) PDFs: rare	normal
3. Moderately shocked	PDFs: $\{10\bar{1}3\}$	PFs: $\{10\bar{1}1\}$, (0001) rare PDFs: $\{11\bar{2}2\}$, $\{11\bar{2}1\}$, (0001), $\{10\bar{1}0\}$+$\{11\bar{2}1\}$, $\{10\bar{1}1\}$, $\{21\bar{3}1\}$, $\{51\bar{6}1\}$	normal or slightly reduced refractive indices
4. Strongly shocked	PDFs: $\{10\bar{1}2\}$ $\{10\bar{1}3\}$	PFs: rare or absent PDFs: $\{11\bar{2}2\}$, $\{11\bar{2}1\}$, (0001), $\{10\bar{1}0\}$+$\{11\bar{2}1\}$, $\{10\bar{1}1\}$, $\{21\bar{3}1\}$, $\{51\bar{6}1\}$	reduced refractive indices (1.546–1.48)
5. Very strongly shocked	PDFs: $\{10\bar{1}2\}$ $\{10\bar{1}3\}$	none	reduced refractive indices (<1.48)

After Stöffler and Langenhorst (1994)
[a]PF = planar fractures; PDF = planar deformation features

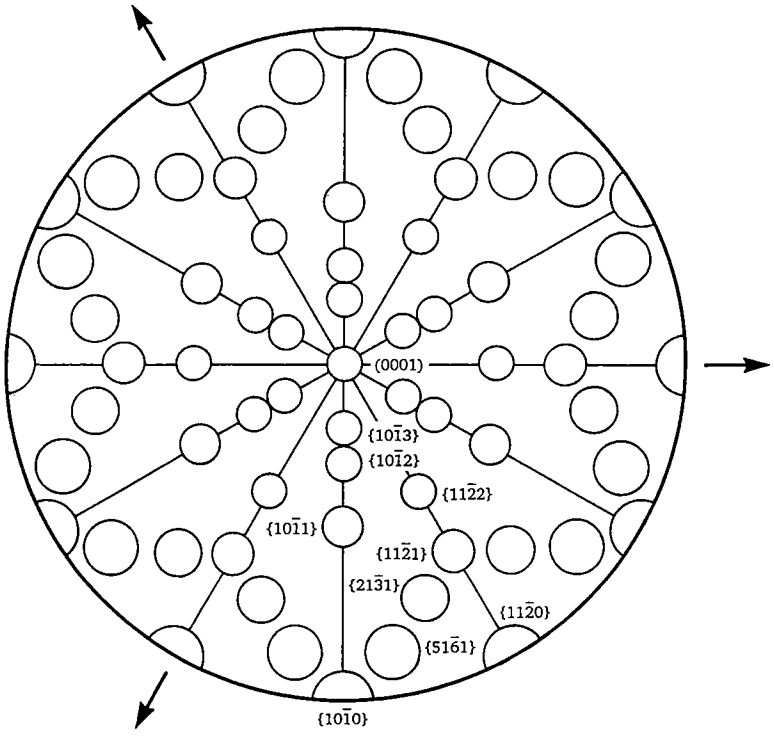

Figure 9. Standard stereographic projection (lower hemisphere) of rational crystallographic planes in α-quartz, which is used to index crystallographic planes of PDFs based on universal-stage measurements. The arrows indicate the three a-axes of quartz, and the c-axis (the (0001) plane) is in the center of the projection. Also indicated are the low Miller indices in a part of the diagram (other indices can be derived from crystal symmetry). The circles are about 5° in diameter and indicate the accuracy of the U-stage measurements (see, e.g., Engelhardt and Bertsch, 1969).

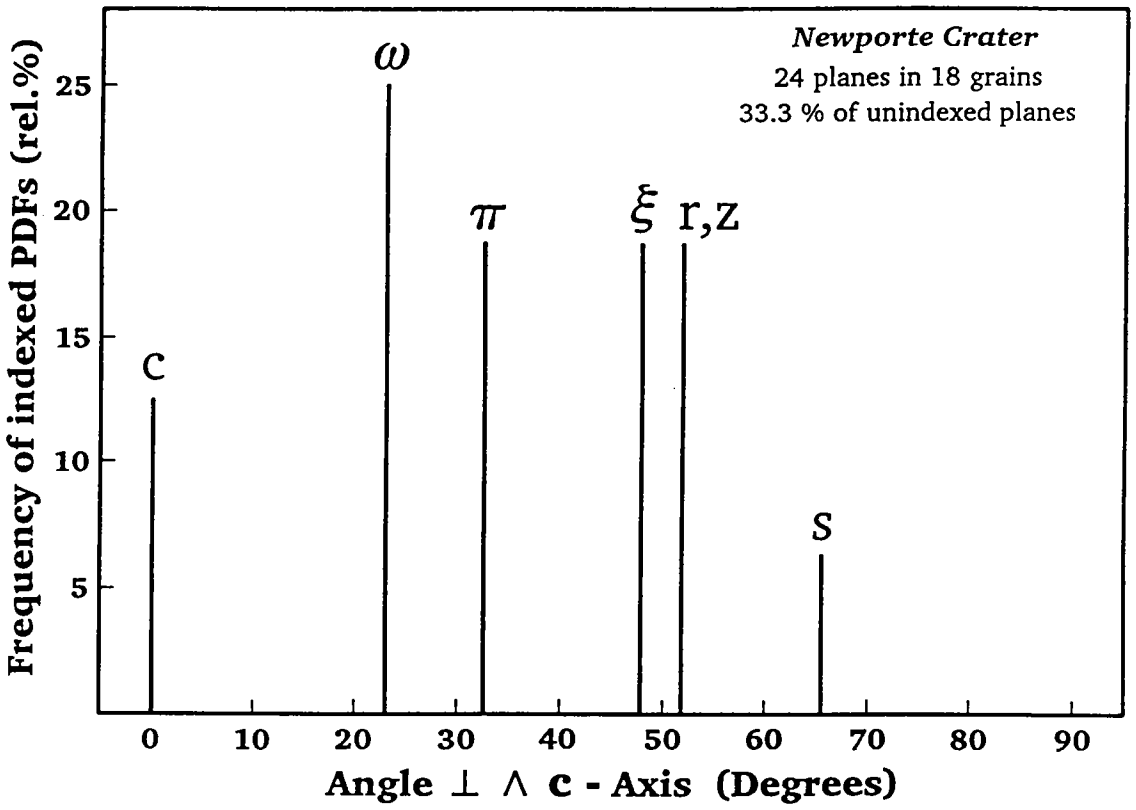

Figure 10. Crystallographic orientation of PDFs in quartz from the Newporte (North Dakota) impact structure, shown as a histogram giving the frequency of indexed PDFs vs. angle between c-axis and poles of PDFs, without plotting unindexed planes (see Grieve and Therriault, 1995); the shock-characteristic orientations (0001), $\{10\bar{1}3\}$, $\{10\bar{1}2\}$, $\{11\bar{2}2\}$, $\{10\bar{1}1\}$, $\{01\bar{1}1\}$, and $\{11\bar{2}1\}$ (*c*, ω, π, ξ, *r*,*z*, and *s*, respectively), are dominating. (After Koeberl and Reimold, 1995b.)

show also an inverse relationship with shock pressure in the 25 to 35 GPa range (Fig. 13). At about 35 GPa, isotropization (formation of diaplectic quartz glass) occurs. Figure 13 also indicates that with increasing shock pressure, the birefringence (n_ω–n_ε) decreases. Still other properties of shocked minerals can be used to either confirm a shock history or calibrate shock pressures. For example, intensity and wavelength of infrared absorption bands, the electron paramagnetic resonance, and peak width in a ^{29}Si magic-angle-spinning nuclear magnetic resonance (NMR) spectrum all depend in a quantitative way on the shock pressure (e.g., Boslough and others, 1995; references in Stöffler and Langenhorst, 1994).

Diaplectic Glass

At shock pressures in excess of about 30 GPa, diaplectic glass is formed (Table 1), which has been found at numerous impact craters. It is an isotropic phase that preserves the crystal habit, original crystal defects, and, in some cases, planar features. It forms without melting by solid-state transformation and has been described as a phase "intermediate between crystalline and normal glassy phases" (Stöffler and Hornemann, 1972). For example, maskelynite forms from feldspar. Diaplectic glass has a refractive index that is slightly lower, and a density that is slightly higher, than that of synthetic quartz glass. At pressures that exceed about 50 GPa, lechatelierite, a mineral melt, forms by fusion of quartz. Other minerals also undergo melting (fusion) at similar pressures. This complete melting is not the same process that results in the formation of diaplectic glass. The distinction between diaplectic glass and lechatelierite (both after quartz) was described by Stöffler and Hornemann (1972) and Stöffler and Langenhorst (1994).

High-Pressure Polymorphs

Another form of shock deformation is phase transitions to high-pressure polymorphs of minerals in a solid-state transformation process. Such transformation can be predicted from Hugoniot data. Many minerals form metastable high-pres-

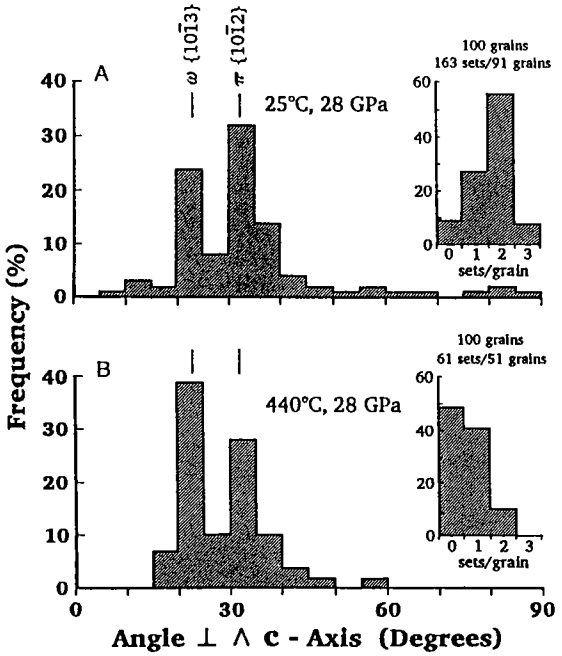

Figure 11. Histograms with crystallographic orientation of PDFs in quartz from Hospital Hill quartzite, used in shock experiments, showing the dependency of the orientations on the preshock temperature (after Huffman and others, 1993). (A) Preshock temperature 25 °C, shock pressure 28 GPa. (B) Preshock temperature 440 °C, shock pressure 28 GPa. The main difference between the data sets is that about half of the quartz grains in the high-temperature experiment remain unshocked, whereas in the low-temperature experiment, almost all quartz grains are shocked.

sure phases (Stöffler, 1972), including (density in g/cm^3 is given in parentheses) stishovite (4.23) and coesite (2.93) from quartz (2.65), jadeite (3.24) from plagioclase (2.63 to 2.76), majorite (3.67) from pyroxene (3.20 to 3.52), and ringwoodite (3.90) from olivine (3.22 to 4.34). In contrast to expectations from the equilibrium phase diagram of quartz, stishovite forms at lower pressures than coesite, probably because stishovite forms directly during shock compression, whereas coesite crystallizes during pressure release.

The formation probabilities and conditions for these phases are strongly dependent on the porosity of the target rocks. Although stishovite has never been found in any natural, non-impact-related rocks, there are rare findings of coesite in metamorphic rocks and kimberlites. However, coesite within metamorphic rocks occurs as large single crystals within, or associated with, high-pressure minerals of metamorphic or volcanic origin, but never associated with quartz. On the other hand, impact-derived coesite occurs as fine-grained, colorless to brownish, polycrystalline aggregates of up to 200 μm in size, which are usually embedded in diaplectic quartz or, rarely, in nearly isotropic shocked quartz. In addition to morphological differences, shock-produced coesite occurs in a disequilibrium assemblage of quartz + coesite + stishovite + glass (see also Grieve and others, 1996).

In addition to high-pressure phases of rock-forming minerals, impact-derived diamonds (the high-pressure polymorph of carbon) have also been found at various craters. These diamonds form from carbon in the target rocks, mainly graphite-bearing (e.g., graphitic gneiss) or less commonly coal-bearing rocks (Koeberl and others, 1995a). Impact diamonds commonly preserve the crystal habit of their precursor material, which is mostly graphite. The diamonds that formed after graphite are called "apographitic" diamonds. Many of them were found to contain up to several 10 vol% lonsdaleite, the rare hexagonal diamond polymorph.

Mineral and Rock Melts

At pressures in excess of about 60 GPa, rocks undergo complete (bulk) melting to form impact

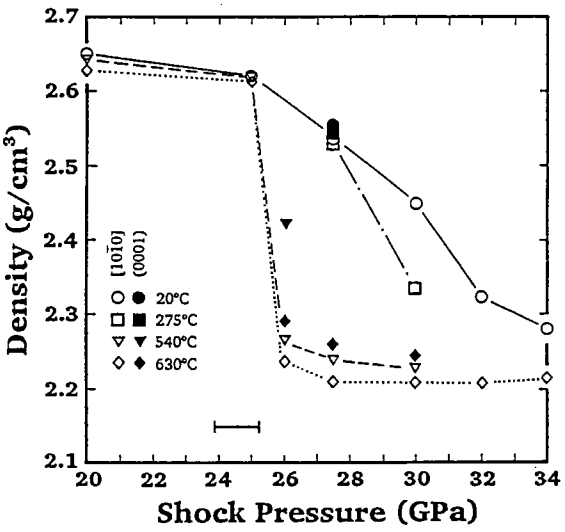

Figure 12. Densities of experimentally shocked quartz crystals at various preshock temperatures (20, 275, 540, and 630 °C), for two different directions of the shock wave relative to the c-axis of the quartz crystal (after Langenhorst, 1993). The measurement error for the shock pressure is indicated by the bar at the bottom of the diagram; the error for the density is smaller than the symbols. The starting value at the upper left of the diagram represents the density of crystalline quartz; the value marked by the diamond at the right side of the diagram marks the density of synthetic quartz glass.

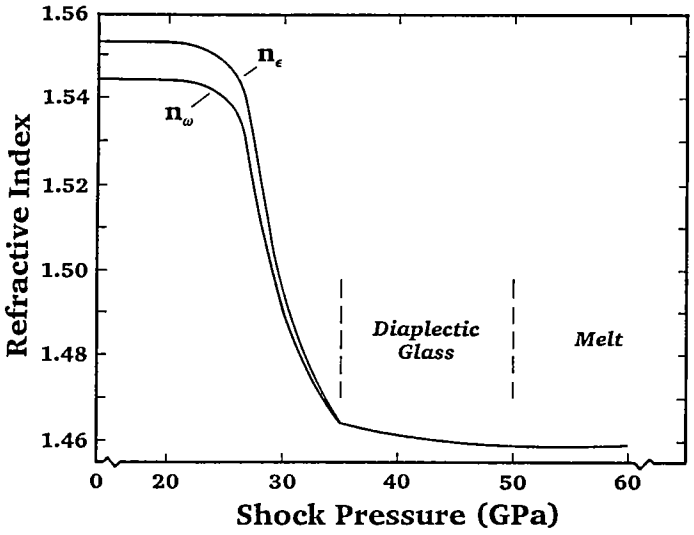

Figure 13. Relationship of refractive index to shock pressure for experimentally shocked quartz (shock front parallel to {10$\bar{1}$0}, i.e., polar angle 90° to c-axis). Preshock temperature of quartz 20 °C. The lower curve is given for the ordinary ray, and the upper curve marks the extraordinary ray in quartz. A smooth and continuous decrease in the refractive index between about 25 and 35 GPa is obvious, followed by isotropization (diaplectic glass) and melting (lechatelierite). (After Stöffler and Langenhorst, 1994.)

melts (see Table 1). The melts can reach very high temperatures because of the passage of shock waves that generate temperatures far beyond those commonly encountered in normal crustal processes or in volcanic eruptions. The very high temperatures are indicated by the presence of inclusions of high-temperature minerals, such as lechatelierite, which forms from pure quartz at temperatures of >1700 °C (see above), or baddeleyite, which is the thermal decomposition product of zircon, forming at a temperature of about 1900 °C. Impact melts may also undergo a phase of superheating (i.e., staying liquid even though the vaporization temperature has been exceeded) at temperatures of 10,000 °C or higher (e.g., Jakes and others, 1992). Depending on the initial temperature, the location within the crater, the composition of the melt, and the speed of cooling, impact melts either form impact glasses (if they cool fast enough) or, more commonly, (mostly) fine-grained impact-melt rocks (if they cool more slowly). Impact-melt rocks are also found in suevitic breccias in the form of melt clasts. Impact-melt rocks contain clasts of shocked minerals or lithic clasts (Fig. 14).

As glasses are metastable supercooled liquids, impact glasses slowly recrystallize (if dissolution is not acting faster), at a rate that depends on the composition of the glass and postimpact environmental conditions. Therefore, impact glasses are more commonly found at young impact craters than at old impact structures. Very fine grained recrystallization textures are often characteristic of devitrified impact glasses (Fig. 14A,B). Impact glasses have chemical and isotopic compositions that are very similar to those of individual target rocks or mixtures of several rock types. For example, it is possible to use the rare earth element (REE) distribution patterns or the Rb-Sr isotopic composition, which are identical to those of the (often sedimentary or metasedimentary) target rocks, to distinguish the impact-melt rocks from intrusive or volcanic rocks (e.g., Blum and Chamberlain, 1992; Blum and others, 1993). Furthermore, impact glasses have much lower water contents (about 0.001–0.05 wt%) than volcanic or other natural glasses (e.g., Koeberl, 1992b). Detailed descriptions of impact melts and glasses and their characteristics and compositions are discussed by, for example, El Goresy and others (1968), Dence (1971), Stöffler (1984), Koeberl (1986,1992a,b), and references therein.

Impact melts and glasses (or minerals that have recrystallized from the melt; e.g., Krogh and others, 1993; Izett and others, 1993) have another important use, as they often are the most suitable material for the dating of an impact structure. The methods most commonly used for dating of impact-melt rocks or glasses include the K-Ar, ^{40}Ar-^{39}Ar, fission-track, Rb-Sr, Sm-Nd, or U-Th-Pb isotope methods. However, dating impact craters is complicated and tedious and, if not done with utmost care, can easily lead to erroneous results (see, e.g., Bottomley and others, 1990, and Deutsch and Schärer, 1994, for reviews of methods of impact crater dating).

GEOCHEMISTRY AND DETECTION OF METEORITIC COMPONENTS IN IMPACTITES

No meteorites have been found at most meteorite impact craters. This fact may seem a contradiction, but it follows as a logical consequence of the physics of an impact event. A shock wave, similar to the one that penetrates through the target, also passes through the meteoritic impactor and, within fractions of a second, vaporizes most or all

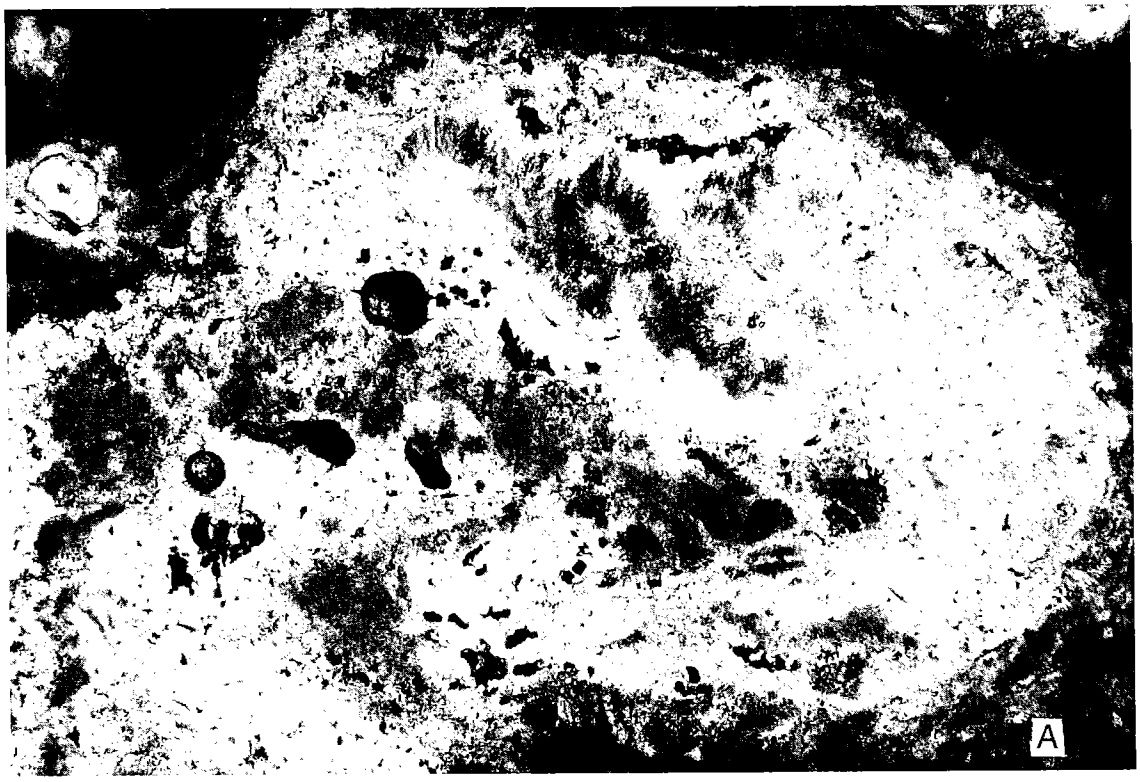

Figure 14. Photomicrographs of impact-melt rocks. A *(above)*—Largely melted quartzitic clast in flow-banded, extremely fine grained, melt matrix, in sample 277.8 from drill core M8, Manson impact structure, Iowa (see Koeberl and others, 1996a); note the fine, feathery recrystallization texture (width of field of view, 2.2 mm; parallel polarizers). B *(facing page)*—Impact-melt breccia 9018.1 from the Ames structure, Oklahoma, Nicor no. 18-4 Chestnut core, depth 2,748.7 m, with fractured and shocked mineral grains set in a finer-grained matrix, showing feathery spherulitic devitrification texture in center and upper right and a diaplectic quartz glass grain on the upper left (width of field of view, 3.4 mm; crossed polarizers; courtesy W. U. Reimold). C *(facing page)*—Aphanitic impact-melt breccia with K-feldspar clasts set in a fine-grained matrix, sample 1341.5 from the Exmore drill core, Chesapeake Bay impact structure, Virginia (see Poag and others, 1994; Koeberl and others, 1995b,1996c; width of field of view, 3.4 mm; crossed polarizers).

of the projectile. Only during the impact of small objects (less than about 40 m in diameter, depending on impact angle and velocity) may a small fraction of the initial mass of the meteorite survive, because of either spallation during entry into the atmosphere or lower impact velocity resulting from atmospheric drag. The cutoff diameter of impact craters at which some fraction of meteoritic material may be preserved is about 1 to 1.5 km. Thus, even under optimistic conditions, meteoritic fragments are preserved at only very young and small craters. The absence of meteorite fragments can, therefore, not be used as evidence against an impact origin of a crater structure.

A more generally applicable impact-diagnostic method is the detection of geochemical traces of the meteoritic projectile in target rocks. Such detection allows establishment of the impact origin for a crater structure. The meteoritic projectile undergoes vaporization in the early phases of crater formation. A small amount of the meteoritic vapor is incorporated with the much larger quantity of target-rock vapor and melt, which later forms impact-melt rocks, melt breccias, or glass. In most cases, the contribution of meteoritic matter to these impactite lithologies is very small (commonly $<<1\%$), leading to only slight chemical changes in the resulting impactites. Only elements that have high abundances in meteorites, but low abundances in terrestrial crustal rocks, can be used to detect such a meteoritic component. During the past two decades, studies of the abundances and interelement ratios of the siderophile elements, such as Cr, Co, Ni, and, especially, the platinum-group elements (PGEs) have been used for these investigations (see, e.g., Morgan and others, 1975; Palme, 1982; Evans and others, 1993; and references therein). However, the use of el-

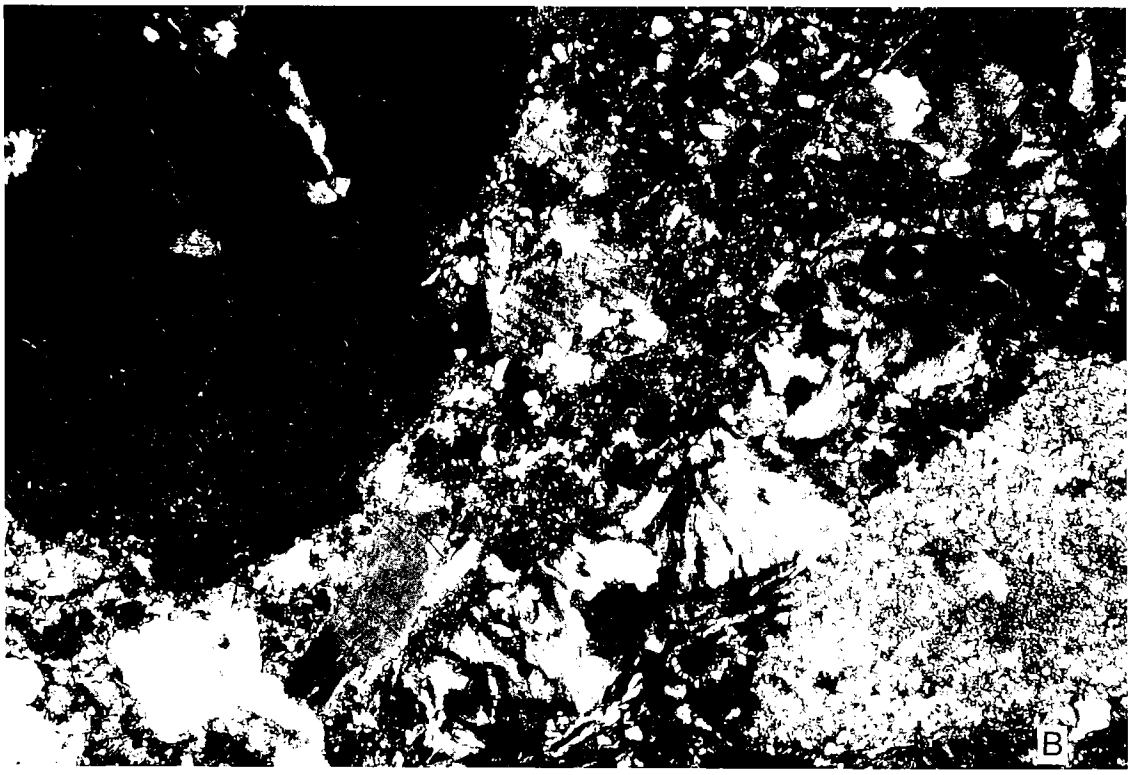

Figure 14B.

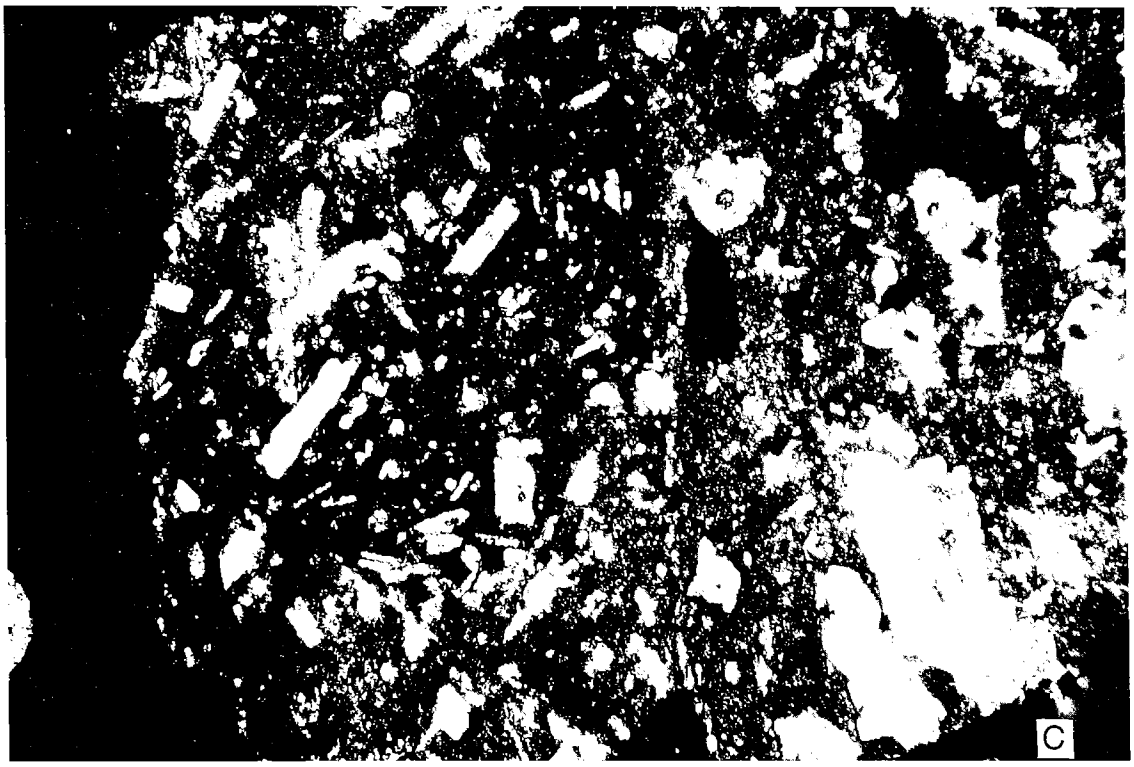

Figure 14C.

emental abundances does not necessarily lead to unambiguous results, as ultramafic rocks or ore minerals may be present among the target rocks, resulting in elevated PGE abundances. Another complication is the possible fractionation of the siderophile elements in the impact melt while it is still molten. This effect may be significant in larger craters, because there the melt can stay hot for many thousand years. Different mineral phases, such as sulfides or oxides (e.g., magnetite, chromite), may take up various proportions of the PGEs or other siderophile elements, leading to an irregular distribution of these elements and possibly fractionated interelement ratios and patterns. Such irregular distribution of siderophiles is known from, for example, the East and West Clearwater impact structures (Palme and others, 1979) and the Chicxulub impact structure (Koeberl and others, 1994c; Schuraytz and others, 1996). Hydrothermal processes associated with the hot impact melt may also change PGE abundances.

The use of the Re-Os isotope system has numerous advantages over the use of elemental abundances of the PGEs. The Re-Os isotope method is superior with respect to detection limit and selectivity, as discussed by Koeberl and Shirey (1993) and Koeberl and others (1994a,b). In principle, the abundances of Re and Os and the $^{187}Os/^{188}Os$ isotope ratios, which are measured by very sensitive mass spectrometric techniques, allow one to distinguish the isotopic signatures of meteoritic and terrestrial Os. Meteorites (and the terrestrial mantle) have much higher (by factors of 10^4 to 10^5) PGE contents than terrestrial crustal rocks. In addition, meteorites have relatively low Re and high Os abundances, resulting in Re/Os ratios less or equal to 0.1, whereas the Re/Os ratio of terrestrial crustal rocks is usually no less than 10. More important even, the $^{187}Os/^{188}Os$ isotope ratios for meteorites and terrestrial crustal rocks are significantly different.

^{187}Os is formed from the β-decay of ^{187}Re (with a half-life of 42.3 ± 1.3 b.y.). Thus, because of the high Re and low Os concentrations in old crustal rocks, their $^{187}Os/^{188}Os$ ratio increases rapidly with time. The present-day $^{187}Os/^{188}Os$ ratio of mantle rocks is about 0.13. Meteorites also have low $^{187}Os/^{188}Os$ ratios of about 0.11 to 0.18. Os is much more abundant in meteorites than Re, leading to only small changes in the meteoritic $^{187}Os/^{188}Os$ ratio with time. Because of the high Os abundances in meteorites, the addition of a minute meteoritical contribution to the crustal target rocks leads to an almost complete change of their Os isotopic signature in the resulting impact melt or breccia (see Fig. 15 for an example). For details about this method, see Koeberl and Shirey (1993, 1996,1997) and Koeberl and others (1994a,b). Like studies of shock metamorphism, Re-Os isotopic measurements of target rocks and impactites may provide good evidence for an impact origin.

CONCLUSIONS

Impact cratering still remains one of the least appreciated geologic processes, even though, over the past three decades, researchers have studied impact cratering and craters in nature, in the laboratory, and by computer modeling. Identification of further impact structures on Earth can only be achieved with diligent and careful investigations. Impact crater research is an excellent example to illustrate the necessity—and success—of interdisciplinary studies. This paper was aimed at describing how mineralogical and geochemical studies should be applied to the identification and characterization of impact craters and impact-derived rocks. As the discussions regarding the impact origin of the Ames structure (see papers in this volume) or the relationship of an impact to the K/T boundary have illustrated (see, e.g., Silver and Schultz, 1982; Sharpton and Ward, 1990; Ryder and others, 1996), there are still lots of misconceptions and a lack of understanding of the mineralogical and geochemical characteristics of shocked rocks. Thus, it is essential that the proper methods for identifying impact craters are understood and used before drawing any conclusions regarding the impact origin of a geologic structure.

ACKNOWLEDGMENTS

Many colleagues have helped with information and references or have provided various other support; I am especially grateful to B. Bohor (U.S. Geological Survey, Denver), B. M. French (Smithsonian Institution, Washington), and R. A. F. Grieve (Geological Survey of Canada, Ottawa). I am also grateful to D. Jalufka for drafting the figures, and B. M. French and W. U. Reimold for detailed comments on the manuscript. I thank K. Johnson and J. Campbell for the invitation to contribute to the symposium, for which this paper is part of the proceedings. Parts of this study were supported by the Austrian Fonds zur Förderung der wissenschaftlichen Forschung, Project P08794-GEO.

REFERENCES CITED

Alexopoulos, J. S.; Grieve, R. A. F.; and Robertson, P. B., 1988, Microscopic lamellar deformation features in quartz: discriminative characteristics of shock-generated varieties: Geology, v. 16, p. 796–799.

Alvarez, L. W.; Alvarez, W.; Asaro, F.; and Michel, H. V., 1980, Extraterrestrial cause for the Cretaceous-Tertiary extinction: Science, v. 208, p. 1095–1108.

Blum, J. D.; and Chamberlain, C. P., 1992, Oxygen isotope constraints on the origin of impact glasses from the Cretaceous-Tertiary boundary: Science, v. 257, p. 1104–1107.

Blum, J. D.; Chamberlain, C. P.; Hingston, M. P.;

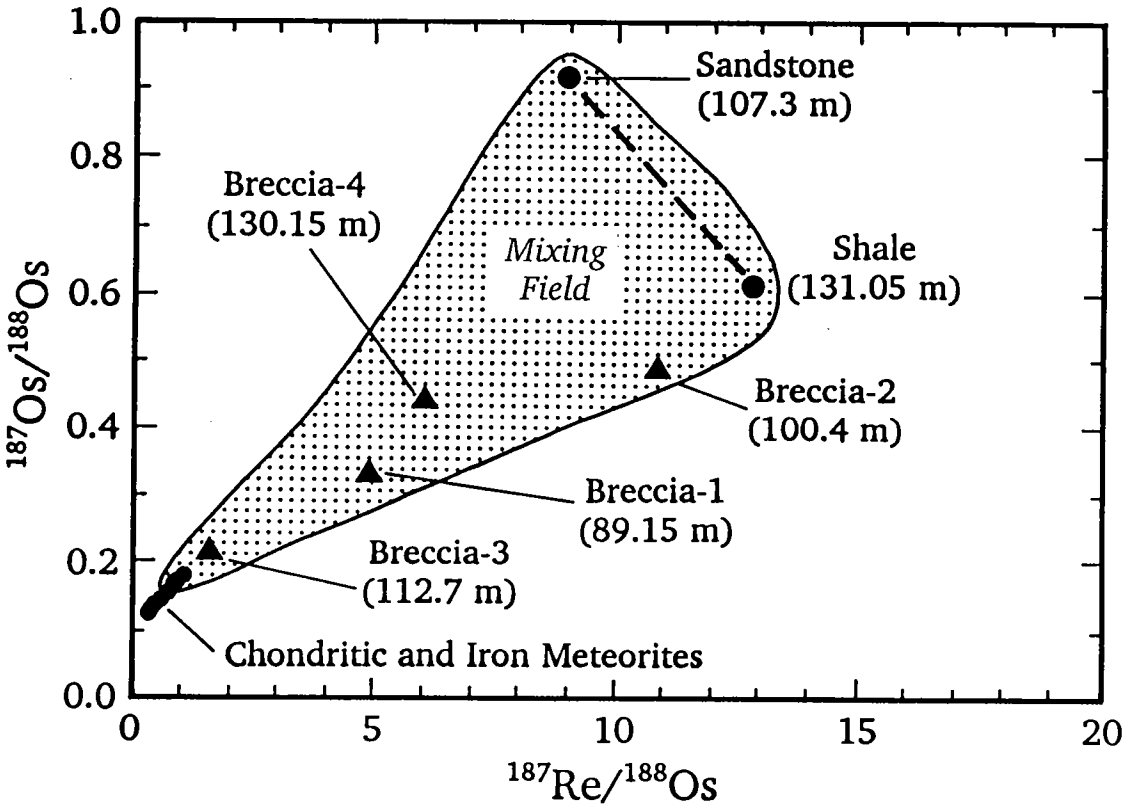

Figure 15. Ratios of $^{187}Os/^{188}Os$ vs. $^{187}Re/^{188}Os$ for target rocks (shale and sandstone) of the Kalkkop impact crater, South Africa, in comparison with data for four impact breccias (solid triangles) and the data array for chondritic and iron meteorites (small solid dots). The sample depths in the drill core are given as well (after Koeberl and others, 1994b). The dotted area marks the mixing field between target rocks and meteorites. All impact breccias fall within this mixing field; breccia-3 plots very close to the meteorite data array, indicating more meteoritic contamination than any other breccia, which is in good agreement with the high Os content of this sample (about 0.2 ppb). In addition to distinct differences in the Os isotope composition, the Os content of the target rocks, at about 0.02 ppb, is about 10 times lower than the Os content of the breccias.

Koeberl, C.; Marin, L. E.; Schuraytz, B. C.; and Sharpton, V. L., 1993, Isotopic comparison of K-T boundary impact glass with melt rock from the Chicxulub and Manson impact structures: Nature, v. 364, p. 325–327.

Bohor, B. F.; Foord, E. E.; Modreski, P. J.; and Triplehorn, D. M., 1984, Mineralogical evidence for an impact event at the Cretaceous/Tertiary boundary: Science, v. 224, p. 867–869.

Bohor, B. F.; Modreski, P. J.; and Foord, E. E., 1987, Shocked quartz in the Cretaceous/Tertiary boundary clays: evidence for global distribution: Science, v. 236, p. 705–708.

Boslough, M. B.; and Asay, J. R., 1993, Basic principles of shock compression, *in* Asay, J. R.; and Shahinpoor, M. (eds.), High-pressure shock compression of solids: Springer-Verlag, Berlin, p. 7–42.

Boslough, M. B.; Cygan, R. T.; and Izett, G. A., 1995, NMR spectroscopy of quartz from the K/T boundary: shock-induced peak broadening, dense glass, and coesite: Lunar and Planetary Science, v. 26, p. 149–150.

Bottomley, R. J.; York, D.; and Grieve, R. A. F., 1990, $^{40}Argon$-$^{39}Argon$ dating of impact craters: Proceedings of the 20th Lunar and Planetary Science Conference, p. 421–431.

Chapman, C. R.; and Morrison, D., 1994, Impacts on the Earth by asteroids and comets: assessing the hazard: Nature, v. 367, p. 33–40.

de Silva, S. L.; Wolff, J. A.; and Sharpton, V. L., 1990, Explosive volcanism and associated pressures: implications for models of endogenic shocked quartz, *in* Sharpton, V. L.; and Ward, P. D. (eds.), Global catastrophes in Earth history: Geological Society of America Special Paper 247, p. 139–145.

Dence, M. R., 1971, Impact melts: Journal of Geophysical Research, v. 76, p. 5525–5565.

Deutsch, A.; and Schärer, U., 1994, Dating terrestrial impact events: Meteoritics, v. 29, p. 301–322.

Dietz, R. S., 1968, Shatter cones in cryptoexplosion structures, *in* French, B. M.; and Short, N. M. (eds.), Shock metamorphism of natural materials: Mono Book Corp., Baltimore, p. 267–285.

El Goresy, A.; Fechtig, H.; and Ottemann, T., 1968, The opaque minerals in impactite glasses, *in* French, B. M.; and Short, N. M., (eds.), Shock metamorphism of natural materials: Mono Book Corp., Baltimore, p. 531–554.

Emmons, R. C., 1943, The universal stage (with five axes of rotation): Geological Society of America Memoir 8, 205 p.

Engelhardt, W. v.; and Bertsch, W., 1969, Shock induced planar deformation structures in quartz from the Ries crater, Germany: Contributions to Mineralogy and Petrology, v. 20, p. 203–234.

Evans, N. J.; Gregoire, D. C.; Grieve, R. A. F.; Goodfellow, W. D.; and Veizer, J., 1993, Use of platinum-group elements for impactor identification: terrestrial impact craters and Cretaceous-Tertiary boundary: Geochimica et Cosmochimica Acta, v. 57, p. 3737–3748.

French, B. M., 1968, Shock metamorphism as a geological process, *in* French, B. M.; and Short, N. M. (eds.), Shock metamorphism of natural materials: Mono Book Corp., Baltimore, p. 1–17.

_____ 1990, Absence of shock-metamorphic effects in the Bushveld complex, South Africa: results of an intensive search: Tectonophysics, v. 171, p. 287–301.

French, B. M.; and Short, N. M. (eds.), 1968, Shock metamorphism of natural materials: Mono Book Corp., Baltimore, 644 p.

Gault, D. E.; Quaide, W. L.; and Oberbeck, V. R., 1968, Impact cratering mechanics and structures, *in* French, B. M.; and Short, N. M. (eds.), Shock metamorphism of natural materials: Mono Book Corp., Baltimore, p. 87–99.

Glen, W., 1994, The mass extinction debates: Stanford University Press, Stanford, California, 370 p.

Goltrant, O.; Cordier, P.; and Doukhan, J. C., 1991, Planar deformation features in shocked quartz: a transmission electron microscopy investigation: Earth and Planetary Science Letters, v. 106, p. 103–115.

Gratz, A. J.; Nellis, W. J.; Christie, J. M.; Brocious, W.; Swegle, J.; and Cordier, P., 1992a, Shock metamorphism of quartz with initial temperatures −170 to +1000°C: Physical Chemistry of Minerals, v. 19, p. 267–288.

Gratz, A. J.; Nellis, W. J.; and Hinsey, N. A., 1992b, Laboratory simulation of explosive volcanic loading and implications for the cause of the K/T boundary: Geophysical Research Letters, v. 19, p. 1391–1394.

Grieve, R. A. F., 1987, Terrestrial impact structures: Annual Reviews of Earth and Planetary Science, v. 15, p. 245–270.

_____ 1991, Terrestrial impact: the record in the rocks: Meteoritics, v. 26, p. 175–194.

_____ 1997, Terrestrial impact structures: basic characteristics and economic significance, with emphasis on hydrocarbon production, in Johnson, K. S.; and Campbell, J. A. (eds.), Ames structure in northwest Oklahoma and similar features: origin and petroleum production (1995 symposium): Oklahoma Geological Survey Circular 100 [this volume], p. 3–16.

Grieve, R. A. F.; and Shoemaker, E. M., 1994, Terrestrial impact cratering, *in* Gehrels, T. (ed.), Hazards due to comets and asteroids: University of Arizona Press, Tucson, p. 417–462.

Grieve, R. A. F.; and Therriault, A. M., 1995, Planar deformation features in quartz: target effects: Lunar and Planetary Science, v. 26, p. 515–516.

Grieve, R. A. F.; Langenhorst, F.; and Stöffler, D., 1996, Shock metamorphism in nature and experiment; II. Significance in geoscience: Meteoritics and Planetary Science, v. 31, p. 6–35.

Hörz, F., 1968, Statistical measurements of deformation structures and refractive indices in experimentally shock loaded quartz, *in* French, B. M.; and Short, N. M. (eds.), Shock metamorphism of natural materials: Mono Book Corp., Baltimore, p. 243–253.

_____ 1982, Ejecta of the Ries crater, Germany, *in* Silver, L. T.; and Schultz, P. H. (eds.), Geological implications of impacts of large asteroids and comets on the Earth: Geological Society of America Special Paper 190, p. 39–55.

Hörz, F.; Ostertag, R.; and Rainey, D. A., 1983, Bunte breccia of the Ries: continuous deposits of large impact craters: Reviews of Geophysics and Space Physics, v. 21, p. 1667–1725.

Hoyt, W. G., 1987, Coon Mountain controversies: University of Arizona Press, Tucson, 442 p.

Huffman, A. R.; Brown, J. M.; Carter, N. L.; and Reimold, W. U., 1993, The microstructural response of quartz and feldspar under shock loading at variable temperatures: Journal of Geophysical Research, v. 98, p. 22171–22197.

Izett, G. A.; Cobban, W. A.; Obradovich, J. D.; and Kunk, M. J., 1993, The Manson impact structure: ^{40}Ar-^{39}Ar age and its distal impact ejecta in the Pierre Shale in southeastern South Dakota: Science, v. 262, p. 729–732.

Jakes, P.; Sen, S.; Matsuishi, K.; Reid, A. M.; King, E. A.; and Casanova, I., 1992, Silicate melts at super liquidus temperatures: reduction and volatilization: Lunar and Planetary Science, v. 23, p. 599–600.

Kieffer, S. W.; and Simonds, C. H., 1980, The role of volatiles and lithology in the impact cratering process: Reviews of Geophysics and Space Physics, v. 18, p. 143–181.

Koeberl, C., 1986, Geochemistry of tektites and impact glasses: Annual Reviews of Earth and Planetary Science, v. 14, p. 323–350.

_____1992a, Geochemistry and origin of Muong Nong–type tektites: Geochimica et Cosmochimica Acta, v. 56, p. 1033–1064.

_____1992b, Water content of glasses from the K/T boundary, Haiti: indicative of impact origin: Geochimica et Cosmochimica Acta, v. 56, p. 4329–4332.

Koeberl, C.; and Anderson, R. R., 1996, Manson and company: impact structures in the United States, *in* Koeberl, C.; and Anderson, R. R. (eds.), The Manson impact structure, Iowa: anatomy of an

impact crater: Geological Society of America Special Paper 302, p. 1–29.
Koeberl, C.; and Reimold, W. U., 1995a, Shock metamorphism at the Red Wing Creek structure, North Dakota: confirmation of impact origin: Lunar and Planetary Science, v. 26, p. 769–770.
_____1995b, The Newporte impact structure, North Dakota: Geochimica et Cosmochimica Acta, v. 59, p. 4747–4767.
Koeberl, C.; and Shirey, S. B., 1993, Detection of a meteoritic component in Ivory Coast tektites with rhenium-osmium isotopes: Science, v. 261, p. 595–598.
_____1996, Re-Os isotope study of rocks from the Manson impact structure, *in* Koeberl, C.; and Anderson, R. R. (eds.), The Manson impact structure, Iowa: anatomy of an impact crater: Geological Society of America Special Paper 302, p. 331–339.
_____1997, Re-Os isotope systematics as a diagnostic tool for the study of impact craters and ejecta: Palaeogeography, Palaeoclimatology, Palaeoecology, in press.
Koeberl, C.; Reimold, W. U.; and Shirey, S. B., 1994a, Saltpan impact crater, South Africa: geochemistry of target rocks, breccias, and impact glasses, and osmium isotope systematics: Geochimica et Cosmochimica Acta, v. 58, p. 2893–2910.
Koeberl, C.; Reimold, W. U.; Shirey, S. B.; and Le Roux, F. G., 1994b, Kalkkop crater, Cape Province, South Africa: confirmation of impact origin using osmium isotope systematics: Geochimica et Cosmochimica Acta, v. 58, p. 1229–1234.
Koeberl, C.; Sharpton, V. L.; Schuraytz, B. C.; Shirey, S. B.; Blum, J. D.; and Marin, L. E., 1994c, Evidence for a meteoritic component in impact melt rock from the Chicxulub structure: Geochimica et Cosmochimica Acta, v. 58, p. 1679–1684.
Koeberl, C.; Masaitis, V. L.; Langenhorst, F.; Stöffler, D.; Schrauder, M.; Lengauer, C.; Gilmour, I.; and Hough, R. M., 1995a, Diamonds from the Popigai impact structure, Russia: Lunar and Planetary Science, v. 26, p. 777–778.
Koeberl, C.; Reimold, W. U.; Brandt, D.; and Poag, C. W., 1995b, Chesapeake Bay crater, Virginia: confirmation of impact origin: Meteoritics, v. 30, p. 528–529.
Koeberl, C.; Reimold, W. U.; Kracher, A.; Träxler, B.; Vormaier, A.; and Körner, W., 1996a, Mineralogical, petrological, and geochemical studies of drill cores from the Manson impact structure, Iowa, *in* Koeberl, C.; and Anderson, R. R. (eds.), The Manson impact structure, Iowa: anatomy of an impact crater: Geological Society of America Special Paper 302, p. 145–219.
Koeberl, C.; Reimold, W. U.; and Brandt, D., 1996b, Red Wing Creek structure, North Dakota: petrographical and geochemical studies, and confirmation of impact origin: Meteoritics and Planetary Science, v. 31, 335–342.
Koeberl, C.; Poag, C. W.; Reimold, W. U.; and Brandt, D., 1996c, Impact origin of Chesapeake Bay structure and the source of North American tektites: Science, v. 271, p. 1263–1266.
Kring, D. A., 1993, The Chicxulub impact event and possible causes of K/T boundary extinctions, *in* Boaz, D.; and Dornan, M. (eds.), Proceedings of the First Annual Symposium of Fossils of Arizona: Mesa Southwest Museum and Southwest Paleontological Society, Mesa, Arizona, p. 63–79.
Krogh, T. E.; Kamo, S. L.; Sharpton, V. L.; Marin, L. E.; and Hildebrand, A. R., 1993, U-Pb ages of single shocked zircons linking distal K/T ejecta to the Chicxulub crater: Nature, v. 366, p. 731–734.
Langenhorst, F., 1993, Hochtemperatur-Stoßwellenexperimente an Quarz-Einkristallen: University of Münster, Germany, unpublished Ph.D. thesis, 126 p.
_____ 1994, Shock experiments on α- and β-quartz; II. Modelling of lattice expansion and amorphization: Earth and Planetary Science Letters, v. 128, p. 683–698.
Leroux, H.; Reimold, W. U.; and Doukhan, J. C., 1994, A T.E.M. investigation of shock metamorphism in quartz from the Vredefort dome, South Africa: Tectonophysics, v. 230, p. 223–239.
Lyons, J. B.; Officer, C. B.; Borella, P. E.; and Lahodynsky, R., 1993, Planar lamellar substructures in quartz: Earth and Planetary Science Letters, v. 119, p. 431–440.
Mark, K., 1987, Meteorite craters: University of Arizona Press, Tucson, 288 p.
Marsh, S. P., 1980, LASL shock Hugoniot data: University of California Press, Berkeley, 658 p.
Marvin, U. B., 1990, Impact and its revolutionary implications for geology, *in* Sharpton, V. L.; and Ward, P. D. (eds.), Global catastrophes in Earth history: Geological Society of America Special Paper 247, p. 147–154.
Medenbach, O., 1985, A new microrefractometer spindle stage and its application: Fortschritte der Mineralogie, v. 63, p. 111–133.
Melosh, H. J., 1989, Impact cratering: a geologic process: Oxford University Press, New York, 245 p.
Milton, D. J., 1977, Shatter cones—an outstanding problem in shock mechanics, *in* Roddy, D. J.; Pepin, R. O.; and Merrill, R. B. (eds.), Impact and explosion cratering: Pergamon Press, New York, p. 703–714.
Morgan, J. W.; Higuchi, H.; Ganapathy, R.; and Anders, E., 1975, Meteoritic material in four terrestrial meteorite craters: Proceedings of the 6th Lunar and Planetary Science Conference, p. 1609–1623.
Morgan, P., 1989, Heat flow in the Earth, *in* James, D. E. (ed.), The encyclopedia of solid earth geophysics: Van Nostrand Reinhold Co., New York, p. 634–646.
Palme, H., 1982, Identification of projectiles of large terrestrial impact craters and some implications for the interpretation of Ir-rich Cretaceous/Tertiary boundary layers, *in* Silver, L. T.; and Schultz, P. H. (eds.), Geological implications of impacts of large asteroids and comets on Earth: Geological Society of America Special Paper 190, p. 223–233.
Palme, H.; Göbel, E.; and Grieve, R. A. F., 1979, The distribution of volatile and siderophile elements in the impact melt of East Clearwater (Quebec): Pro-

ceedings of the 10th Lunar and Planetary Science Conference, p. 2465–2492.
Pilkington, M.; and Grieve, R. A. F., 1992, The geophysical signature of terrestrial impact craters: Reviews of Geophysics, v. 30, p. 161–181.
Poag, C. W.; Powars, D. S.; Poppe, L. J.; and Mixon, R. B., 1994, Meteoroid mayhem in Ole Virginny: source of the North American tektite strewn field: Geology, v. 22, p. 691–694.
Reimold, W. U., 1988, Shock experiments with preheated Witwatersrand quartzite and the Vredefort microdeformation controversy: Lunar and Planetary Science, v. 19, p. 970–971.
_____ 1995, Pseudotachylite in impact structures—generation by friction melting and shock brecciation?: a review and discussion: Earth-Science Reviews, v. 39, p. 247–265.
Reinhard, M., 1931, Universaldrehtischmethoden: Birkhäuser Verlag, Basel, 118 p.
Robertson, P. B.; Dence, M. R.; and Vos, M. A., 1968, Deformation in rock-forming minerals from Canadian craters, in French, B. M.; and Short, N. M. (eds.), Shock metamorphism of natural materials: Mono Book Corp., Baltimore, p. 433–452.
Roddy, D. J.; Pepin, R. O.; and Merrill, R. B. (eds.), 1977, Impact and explosion cratering: Pergamon Press, New York, 1301 p.
Ryder, G.; Fastovsky, D.; and Gartner, S. (eds.), 1996, The Cretaceous-Tertiary event and other catastrophes in Earth history: Geological Society of America Special Paper 307, 576 p.
Schultz, P. H.; Koeberl, C.; Bunch, T.; Grant, J.; and Collins, W., 1994, Ground truth for oblique impact processes: new insight from the Rio Cuarto, Argentina, crater field: Geology, v. 22, p. 889–892.
Schuraytz, B. C.; Lindstrom, D. J.; Marín, L. E.; Martinez, R. R.; Mittlefehldt, D. W.; Sharpton, V. L.; and Wentworth, S. J., 1996, Iridium metal in Chicxulub impact melt: forensic chemistry on the K-T smoking gun: Science, v. 271, p. 1573–1576.
Sclater, J. G.; Jaupart, C.; and Galson, D., 1980, The heat flow through oceanic and continental crust and the heat loss of the Earth: Reviews in Geophysics and Space Physics, v. 18, p. 269–311.
Sharpton, V. L.; and Grieve, R. A. F., 1990, Meteorite impact, cryptoexplosion, and shock metamorphism: a perspective on the evidence at the K/T boundary, *in* Sharpton, V. L.; and Ward, P. D. (eds.), Global catastrophes in Earth history: Geological Society of America Special Paper 247, p. 301–318.
Sharpton, V. L.; and Ward, P. D. (eds.), 1990, Global catastrophes in Earth history: Geological Society of America Special Paper 247, 631 p.
Shoemaker, E. M.; Wolfe, R. F.; and Shoemaker, C. S., 1990, Asteroid and comet flux in the neighborhood of Earth, *in* Sharpton, V. L.; and Ward, P. D. (eds.), Global catastrophes in Earth history: Geological Society of America Special Paper 247, p. 155–170.
Silver, L. T.; and Schultz, P. H. (eds.), 1982, Geological implications of impacts of large asteroids and comets on the Earth: Geological Society of America Special Paper 190, 528 p.
Stöffler, D., 1972, Deformation and transformation of rock-forming minerals by natural and experimental shock processes: 1. Behaviour of minerals under shock compression: Fortschritte der Mineralogie, v. 49, p. 50–113.
_____ 1974, Deformation and transformation of rock-forming minerals by natural and experimental processes: 2. Physical properties of shocked minerals: Fortschritte der Mineralogie, v. 51, p. 256–289.
_____ 1984, Glasses formed by hypervelocity impact: Journal of Non-crystalline Solids, v. 67, p. 465–502.
Stöffler, D.; and Grieve, R. A. F., 1994, Classification and nomenclature of impact metamorphic rocks: a proposal to the IUGS Subcommission on the Systematics of Metamorphic Rocks: Lunar and Planetary Science, v. 25, p. 1347–1348.
Stöffler, D.; and Hornemann, U., 1972, Quartz and feldspar glasses produced by natural and experimental shock: Meteoritics, v. 7, p. 371–394.
Stöffler, D.; and Langenhorst, F., 1994, Shock metamorphism of quartz in nature and experiment: I. Basic observations and theory: Meteoritics, v. 29, p. 155–181.
Stöffler, D.; Deutsch, A.; Avermann, M.; Bischoff, L.; Brockmeyer, P.; Buhl, D.; Lakomy, R.; and Müller-Mohr, V., 1994, The formation of the Sudbury structure, Canada: toward a unified impact model, *in* Dressler, B. O.; Grieve, R. A. F.; and Sharpton, V. L. (eds.), Large meteorite impacts and planetary evolution: Geological Society of America Special Paper 293, p. 303–318.
Wegener, A., 1921, Die Entstehung der Mondkrater: Friedrich Vieweg and Sohn, Braunschweig, 48 p.
Weissman, P. R., 1990, The cometary impactor flux at the Earth, *in* Sharpton, V. L.; and Ward, P. D. (eds.), Global catastrophes in Earth history: Geological Society of America Special Paper 247, p. 171–180.